

FINITE ELEMENT COMPLEXES IN TWO DIMENSIONS

LONG CHEN AND XUEHAI HUANG

ABSTRACT. In this study, two-dimensional finite element complexes with various levels of smoothness, including the de Rham complex, the curldiv complex, the elasticity complex, and the divdiv complex, are systematically constructed. Smooth scalar finite elements in two dimensions are developed based on a non-overlapping decomposition of the simplicial lattice and the Bernstein basis of the polynomial space, with the order of differentiability at vertices being greater than twice that at edges. Finite element de Rham complexes with different levels of smoothness are devised using smooth finite elements with smoothness parameters that satisfy certain relations. Finally, finite element elasticity complexes and finite element divdiv complexes are derived from finite element de Rham complexes by using the Bernstein-Gelfand-Gelfand (BGG) framework. This study is the first work to construct finite element complexes in a systematic way. Moreover, the novel tools developed in this work, such as the non-overlapping decomposition of the simplicial lattice and the discrete BGG construction, can be useful for further research in this field.

1. INTRODUCTION

Hilbert complexes play a fundamental role in the theoretical analysis and the design of stable numerical methods for partial differential equations [5, 2, 3, 12]. Recently in [7] Arnold and Hu have developed a systematical approach to derive new complexes from well-understood differential complexes such as the de Rham complex involving Sobolev spaces. In this work we shall construct two-dimensional finite element complexes with various smoothness in a systematic way, including finite element de Rham complexes, finite element elasticity complexes, and finite element divdiv complexes etc.

We first construct smooth finite elements in two dimensions by a geometric approach, in which the simplicial lattice $\mathbb{T}_k^2 = \{\alpha = (\alpha_0, \alpha_1, \alpha_2) \in \mathbb{N}^{0:2} \mid \alpha_0 + \alpha_1 + \alpha_2 = k\}$ as the multi-index set with sum k is employed. The smoothness (order of differentiability) at vertices and edges are specified by parameters r^v and r^e , respectively. Let \mathcal{T}_h be a triangulation of a domain $\Omega \subset \mathbb{R}^2$ and denote by $\mathbf{r} = (r^v, r^e)$. When $r^v \geq 2r^e$ and $k \geq 2r^v + 1$, we construct C^{r^e} -continuous finite element spaces $\mathbb{V}_k(\mathcal{T}_h; \mathbf{r})$ using a non-overlapping decomposition (partition) of the simplicial lattice \mathbb{T}_k^2 and the Bernstein basis $\{\lambda^\alpha, \alpha \in \mathbb{T}_k^2\}$ of polynomial space \mathbb{P}_k , where λ is the barycentric coordinate. Notice that the C^{r^e} -continuity implies $\mathbb{V}_k(\mathcal{T}_h; \mathbf{r}) \subset H^{r^e+1}(\Omega)$.

We then move to the finite element de Rham complexes with various smoothness which include discrete versions of the de Rham complex, for $r \geq 1$,

$$(1) \quad \mathbb{R} \xrightarrow{C} H^{r+1}(\Omega) \xrightarrow{\text{curl}} \mathbf{H}^r(\Omega; \mathbb{R}^2) \xrightarrow{\text{div}} H^{r-1}(\Omega) \longrightarrow 0,$$

The first author was supported by NSF DMS-1913080 and DMS-2012465. The second author was supported by the National Natural Science Foundation of China Project 12171300 and the Natural Science Foundation of Shanghai 21ZR1480500.

Accepted by SCIENTIA SINICA Mathematica (in Chinese).

and one with mixed regularities, for $r \geq 0, s \geq \max\{r-1, 0\}$,

$$(2) \quad \mathbb{R} \xrightarrow{\subset} H^{r+1}(\Omega) \xrightarrow{\text{curl}} \mathbf{H}^{r,s}(\text{div}, \Omega) \xrightarrow{\text{div}} H^s(\Omega) \longrightarrow 0,$$

where

$$\mathbf{H}^{r,s}(\text{div}, \Omega) := \{\mathbf{v} \in \mathbf{H}(\text{div}, \Omega) : \mathbf{v} \in \mathbf{H}^r(\Omega; \mathbb{R}^2), \text{div } \mathbf{v} \in H^s(\Omega)\}.$$

Obviously (1) is a special case of (2) and also known as the Stokes complex.

Given three integer vectors $\mathbf{r}_0 = (r_0^v, r_0^e)$, $\mathbf{r}_1 = (r_1^v, r_1^e)$, $\mathbf{r}_2 = (r_2^v, r_2^e)$ satisfying $r_1^v \geq 2r_1^e + 1, r_2^v \geq 2r_2^e$ and $\mathbf{r}_0 = \mathbf{r}_1 + 1, \mathbf{r}_1 \geq -1, \mathbf{r}_2 \geq \mathbf{r}_1 \ominus 1$, for k sufficiently large, we devise finite element de Rham complexes of various smoothness

$$(3) \quad \mathbb{R} \xrightarrow{\subset} \mathbb{V}_{k+1}^{\text{curl}}(\mathcal{T}_h; \mathbf{r}_0) \xrightarrow{\text{curl}} \mathbb{V}_k^{\text{div}}(\mathcal{T}_h; \mathbf{r}_1, \mathbf{r}_2) \xrightarrow{\text{div}} \mathbb{V}_{k-1}^{L^2}(\mathcal{T}_h; \mathbf{r}_2) \rightarrow 0,$$

which is a conforming discretization of the de Rham complex (2). The finite element de Rham complex (3) with $\mathbf{r}_0 = \mathbf{r}_1 + 1$ and $\mathbf{r}_2 = \mathbf{r}_1 - 1$ has been developed recently in [28]. We refer to [33, 24] for some nonconforming Stokes complexes modified from conforming finite element de Rham complexes.

By rotation of the vector field and differential operators, we also obtain the finite element de Rham complex involving grad, rot operators:

$$(4) \quad \mathbb{R} \xrightarrow{\subset} \mathbb{V}_{k+1}^{\text{grad}}(\mathcal{T}_h; \mathbf{r}_0) \xrightarrow{\text{grad}} \mathbb{V}_k^{\text{rot}}(\mathcal{T}_h; \mathbf{r}_1, \mathbf{r}_2) \xrightarrow{\text{rot}} \mathbb{V}_{k-1}^{L^2}(\mathcal{T}_h; \mathbf{r}_2) \rightarrow 0,$$

in which the space $\mathbb{V}_k^{\text{rot}}(\mathcal{T}_h; \mathbf{r}_1, \mathbf{r}_2)$ can find applications in the discretization of Maxwell equation or the fourth-order curl problems.

Several existing finite element de Rham complexes in two dimensions are special examples of (3) or (4), and summarized in Table 1.

TABLE 1. Examples of finite element de Rham complexes (3).

$k \geq$	\mathbf{r}_0	\mathbf{r}_1	\mathbf{r}_2	Results
1	(0, 0)	(-1, -1)	(-1, -1)	standard
4	(0, 0)	(-1, -1)	(0, 0)	[30, Section 5.2.1]
4	(2, 1)	(1, 0)	(0, -1)	[22, Section 3]
4	(2, 1)	(1, 0)	(0, 0)	[22, Section 4]
2	(1, 0)	(0, -1)	(-1, -1)	[19, Section 2.2]

Based on finite element de Rham complexes, we use the Bernstein-Gelfand-Gelfand (BGG) framework [7] to construct more finite element complexes. For $\mathbf{r}_1 \geq -1$ and $\mathbf{r}_2 \geq \mathbf{r}_1 \ominus 1$ satisfying $r_1^v \geq 2r_1^e + 2, r_2^v \geq 2r_2^e$, and polynomial degree k sufficiently large, we design the BGG diagram

$$\begin{array}{ccccccc} \mathbb{R} & \xrightarrow{\subset} & \mathbb{V}_{k+2}^{\text{curl}}(\mathbf{r}_1 + 2) & \xrightarrow{\text{curl}} & \mathbb{V}_{k+1}^{\text{div}}(\mathbf{r}_1 + 1) & \xrightarrow{\text{div}} & \mathbb{V}_k^{L^2}(\mathbf{r}_1) \longrightarrow 0 \\ & & & \nearrow \text{id} & & \nearrow -2 \text{sskw} & \\ \mathbb{R}^2 & \xrightarrow{\subset} & \mathbb{V}_{k+1}^{\text{curl}}(\mathbf{r}_1 + 1; \mathbb{R}^2) & \xrightarrow{\text{curl}} & \mathbb{V}_k^{\text{div}}(\mathbf{r}_1, \mathbf{r}_2; \mathbb{M}) & \xrightarrow{\text{div}} & \mathbb{V}_{k-1}^{L^2}(\mathbf{r}_2; \mathbb{R}^2) \longrightarrow \mathbf{0} \end{array}$$

which leads to the finite element elasticity complex

$$(5) \quad \mathbb{P}_1 \xrightarrow{\subset} \mathbb{V}_{k+2}^{\text{curl}}(\mathbf{r}_1 + 2) \xrightarrow{\text{Air}} \mathbb{V}_k^{\text{div}}(\mathbf{r}_1, \mathbf{r}_2; \mathbb{S}) \xrightarrow{\text{div}} \mathbb{V}_{k-1}^{L^2}(\mathbf{r}_2; \mathbb{R}^2) \rightarrow \mathbf{0}.$$

For $\mathbf{r}_1 \geq 0$, $\mathbf{r}_2 \geq \max\{\mathbf{r}_1 - 2, -1\}$, and $k \geq \max\{2r_1^v + 3, 2r_2^v + 3\}$, we build the BGG diagram

$$\begin{array}{ccccccc} \mathbb{R}^2 & \xrightarrow{\subset} & \mathbb{V}_{k+1}^{\text{curl}}(\mathbf{r}_1 + 1; \mathbb{R}^2) & \xrightarrow{\text{curl}} & \mathbb{V}_k^{\text{div div}^+}(\mathbf{r}_1, \mathbf{r}_2; \mathbb{M}) & \xrightarrow{\text{div}} & \mathbb{V}_{k-1}^{\text{div}}(\mathbf{r}_1 - 1, \mathbf{r}_2) \longrightarrow \mathbf{0} \\ & & & \nearrow \text{mskw} & & \nearrow \text{id} & \\ \mathbb{R} & \xrightarrow{\subset} & \mathbb{V}_k^{\text{curl}}(\mathbf{r}_1) & \xrightarrow{\text{curl}} & \mathbb{V}_{k-1}^{\text{div}}(\mathbf{r}_1 - 1, \mathbf{r}_2) & \xrightarrow{\text{div}} & \mathbb{V}_{k-2}^{L^2}(\mathbf{r}_2) \longrightarrow 0 \end{array}$$

which leads to the finite element divdiv complex

$$(6) \quad \mathbf{RT} \xrightarrow{\subset} \mathbb{V}_{k+1}^{\text{curl}}(\mathbf{r}_1 + 1; \mathbb{R}^2) \xrightarrow{\text{sym curl}} \mathbb{V}_k^{\text{div div}^+}(\mathbf{r}_1, \mathbf{r}_2; \mathbb{S}) \xrightarrow{\text{div div}} \mathbb{V}_{k-2}^{L^2}(\mathbf{r}_2) \rightarrow 0,$$

where $\mathbb{V}_k^{\text{div div}^+}(\mathbf{r}_1, \mathbf{r}_2; \mathbb{S}) \subset \mathbf{H}(\text{div div}, \Omega; \mathbb{S}) \cap \mathbf{H}(\text{div}, \Omega; \mathbb{S})$. We refer to Section 5 for details. By a refinement of the BGG diagram, the finite element divdiv complexes presented in [29] and [13] with $\mathbf{r}_1 = (0, -1)$, $\mathbf{r}_2 = (-1, -1)$ are also covered.

Several existing finite element complexes in two dimensions can be viewed as special cases of (5) or (6), and are summarized in Table 2. However, discrete elasticity complexes and rot rot complexes based on the Clough-Tocher split in [20] are constructed using piecewise polynomials as shape functions, which are not covered by (5) and (6).

TABLE 2. Examples of finite element elasticity and finite element divdiv complexes.

Type	$k \geq$	\mathbf{r}_1	\mathbf{r}_2	Results
Elasticity complex (5)	3	(0, -1)	(-1, -1)	[19, Section 6]
Hessian complex (rotation of (5))	5	(0, -1)	(0, 0)	[15, Section 5.1]
divdiv complex (6)	6	(1, 0)	(0, 0)	[15, Section 5.2]
divdiv complex (46)	3	(0, -1)	(-1, -1)	[29, Section 2.3]
divdiv complex (48)	3	(0, -1)	(-1, -1)	[13, Section 3.3]

The rest of this paper is organized as follows. The de Rham complex and BGG framework are reviewed in Section 2. In Section 3 the geometric decomposition of C^m -conforming finite elements in two dimensions is studied. Finite element de Rham complexes with various smoothness are constructed in Section 4. More finite element complexes based on the BGG approach are developed in Section 5.

2. PRELIMINARIES ON HILBERT COMPLEXES

2.1. **Notation.** For scalar function v , denote

$$\text{mskw } v := \begin{pmatrix} 0 & -v \\ v & 0 \end{pmatrix}, \quad \text{curl } v := \left(\frac{\partial v}{\partial x_2}, -\frac{\partial v}{\partial x_1} \right)^\top = (\text{grad } v)^\perp,$$

where $(a, b)^\perp := (b, -a)$ is the 90° rotation clock-wisely, $\text{hess} := \text{grad grad}$, and

$$\text{Air } v := \text{curl curl } v = \begin{pmatrix} \frac{\partial^2 v}{\partial x_2^2} & -\frac{\partial^2 v}{\partial x_1 \partial x_2} \\ -\frac{\partial^2 v}{\partial x_1 \partial x_2} & \frac{\partial^2 v}{\partial x_1^2} \end{pmatrix}.$$

Then $\operatorname{div}(\operatorname{mskw} v) = -\operatorname{curl} v$. For vector function $\mathbf{v} = (v_1, v_2)$, denote

$$\operatorname{rot} \mathbf{v} := \frac{\partial v_2}{\partial x_1} - \frac{\partial v_1}{\partial x_2} = \operatorname{div} \mathbf{v}^\perp.$$

For tensor function $\boldsymbol{\tau} = \begin{pmatrix} \tau_{11} & \tau_{12} \\ \tau_{21} & \tau_{22} \end{pmatrix}$, denote

$$\begin{aligned} \operatorname{sym} \boldsymbol{\tau} &:= \frac{1}{2}(\boldsymbol{\tau} + \boldsymbol{\tau}^\top), \quad \operatorname{skw} \boldsymbol{\tau} := \frac{1}{2}(\boldsymbol{\tau} - \boldsymbol{\tau}^\top), \\ \operatorname{sskw} \boldsymbol{\tau} &:= \operatorname{mskw}^{-1} \circ \operatorname{skw} \boldsymbol{\tau} = \frac{1}{2}(\tau_{21} - \tau_{12}). \end{aligned}$$

By direct calculation, we have

$$(7) \quad \operatorname{div} \mathbf{v} = 2 \operatorname{sskw}(\operatorname{curl} \mathbf{v}), \quad \operatorname{rot} \mathbf{v} = 2 \operatorname{sskw}(\operatorname{grad} \mathbf{v}).$$

2.2. Hilbert complex and exact sequence. A Hilbert complex is a sequence of Hilbert spaces $\{\mathcal{V}_i\}$ connected by a sequence of closed densely defined linear operators $\{d_i\}$

$$(8) \quad 0 \hookrightarrow \mathcal{V}_1 \xrightarrow{d_1} \mathcal{V}_2 \xrightarrow{d_2} \cdots \xrightarrow{d_{n-2}} \mathcal{V}_{n-1} \xrightarrow{d_{n-1}} \mathcal{V}_n \xrightarrow{d_n} 0,$$

satisfying the property $\operatorname{img}(d_i) \subseteq \ker(d_{i+1})$. We will abbreviate Hilbert complexes as complexes. The complex is called an exact sequence if $\ker(d_1) = 0$ and $\operatorname{img}(d_i) = \ker(d_{i+1})$ for $i = 1, \dots, n-1$. Therefore if (8) is exact, d_1 is injective and d_{n-1} is surjective. To save notation, we usually skip the trivial space 0 in the beginning of the complex and use the embedding $\mathcal{V}_1 \xrightarrow{\subset} \mathcal{V}_2$ to indicate d_1 is injective. For more background on Hilbert complexes, we refer to [3].

When the Hilbert spaces are finite-dimensional, to verify the exactness, we rely on the following result on the dimension count.

Lemma 2.1. *Let*

$$(9) \quad \mathcal{V}_0 \xrightarrow{\subset} \mathcal{V}_1 \xrightarrow{d_1} \mathcal{V}_2 \xrightarrow{d_2} \mathcal{V}_3 \longrightarrow 0,$$

be a complex, where \mathcal{V}_i are finite-dimensional linear spaces for $i = 0, \dots, 3$. Assume $\mathcal{V}_0 = \mathcal{V}_1 \cap \ker(d_1)$, and

$$(10) \quad \dim \mathcal{V}_0 - \dim \mathcal{V}_1 + \dim \mathcal{V}_2 - \dim \mathcal{V}_3 = 0.$$

If either $d_1 \mathcal{V}_1 = \mathcal{V}_2 \cap \ker(d_2)$ or $d_2 \mathcal{V}_2 = \mathcal{V}_3$, then complex (9) is exact.

Proof. Given the identity (10) and the relation $\mathcal{V}_0 = \mathcal{V}_1 \cap \ker(d_1)$, we prove the equivalence of $d_1 \mathcal{V}_1 = \mathcal{V}_2 \cap \ker(d_2)$ and $d_2 \mathcal{V}_2 = \mathcal{V}_3$ by dimension count. By $\mathcal{V}_0 = \mathcal{V}_1 \cap \ker(d_1)$,

$$\dim d_1 \mathcal{V}_1 = \dim \mathcal{V}_1 - \dim(\mathcal{V}_1 \cap \ker(d_1)) = \dim \mathcal{V}_1 - \dim \mathcal{V}_0.$$

Then it follows from (10) that

$$\begin{aligned} \dim(\mathcal{V}_2 \cap \ker(d_2)) - \dim d_1 \mathcal{V}_1 &= \dim \mathcal{V}_2 - \dim d_2 \mathcal{V}_2 - \dim \mathcal{V}_1 + \dim \mathcal{V}_0 \\ &= \dim \mathcal{V}_3 - \dim d_2 \mathcal{V}_2, \end{aligned}$$

as required. \square

2.3. The de Rham complex. For a domain $\Omega \subseteq \mathbb{R}^2$, the de Rham complex is

$$(11) \quad \mathbb{R} \xrightarrow{\subset} H^1(\Omega) \xrightarrow{\text{curl}} \mathbf{H}(\text{div}, \Omega) \xrightarrow{\text{div}} L^2(\Omega) \rightarrow 0.$$

When Ω is simply connected, the de Rham complex (11) is exact. By changing smoothness of the Sobolev spaces, we obtain the version (2).

Restricted to one triangle, a polynomial de Rham complex is, for integer $k \geq 1$,

$$(12) \quad \mathbb{R} \xrightarrow{\subset} \mathbb{P}_{k+1}(T) \xrightarrow{\text{curl}} \mathbb{P}_k(T; \mathbb{R}^2) \xrightarrow{\text{div}} \mathbb{P}_{k-1}(T) \rightarrow 0,$$

where $\mathbb{P}_k(T)$ denotes the set of real valued polynomials defined on T of degree less than or equal to k , and $\mathbb{P}_k(T; \mathbb{X}) := \mathbb{P}_k(T) \otimes \mathbb{X}$ for \mathbb{X} being vector space \mathbb{R}^2 , tensor space \mathbb{M} , or symmetric tensor space \mathbb{S} .

The following identity

$$(13) \quad 1 - \binom{k+3}{2} + 2 \binom{k+2}{2} - \binom{k+1}{2} = 0$$

can be verified directly. The relation $\text{curl} \mathbb{P}_{k+1}(T) = \mathbb{P}_k(T; \mathbb{R}^2) \cap \ker(\text{div})$ is due to the fact: if $\text{grad } p \in \mathbb{P}_k(T; \mathbb{R}^2)$, then $p \in \mathbb{P}_{k+1}(T)$, and in two dimensions curl is a rotation of grad . Therefore complex (12) is exact by Lemma 2.1.

2.4. Bernstein-Gelfand-Gelfand construction. Eastwood's work [21] established the relationship between the elasticity complex and the de Rham complex via the Bernstein-Gelfand-Gelfand (BGG) construction [9]. Arnold, Falk, and Winther [4] expanded upon this connection by replicating the same construction in the discrete setting, which they used to reconstruct the finite element elasticity complex from the finite element de Rham complexes, as previously introduced in [8]. While a systematic BGG construction has been developed more recently in [7], our focus in this work is limited to two-dimensional complexes, so we will rely on specific examples rather than the abstract framework in [7].

We stack two de Rham complexes into the BGG diagram

$$(14) \quad \begin{array}{ccccccc} \mathbb{R} & \xrightarrow{\subset} & H^2(\Omega) & \xrightarrow{\text{curl}} & \mathbf{H}^1(\Omega; \mathbb{R}^2) & \xrightarrow{\text{div}} & L^2(\Omega) \longrightarrow 0 \\ & \nearrow & \uparrow \cdot(-\mathbf{x})^\perp & \nearrow \text{id} & \uparrow & \nearrow -2 \text{sskw} & \\ \mathbb{R}^2 & \xrightarrow{\subset} & \mathbf{H}^1(\Omega; \mathbb{R}^2) & \xrightarrow{\text{curl}} & \mathbf{H}(\text{div}, \Omega; \mathbb{M}) & \xrightarrow{\text{div}} & \mathbf{L}^2(\Omega; \mathbb{R}^2) \longrightarrow 0 \end{array},$$

which leads to the elasticity complex

$$(15) \quad \mathbb{P}_1 \xrightarrow{\subset} H^2(\Omega) \xrightarrow{\text{Air}} \mathbf{H}(\text{div}, \Omega; \mathbb{S}) \xrightarrow{\text{div}} \mathbf{L}^2(\Omega; \mathbb{R}^2) \rightarrow \mathbf{0}.$$

By rotation, we also have the Hessian complex

$$\mathbb{P}_1 \xrightarrow{\subset} H^2(\Omega) \xrightarrow{\text{hess}} \mathbf{H}(\text{rot}, \Omega; \mathbb{S}) \xrightarrow{\text{rot}} \mathbf{L}^2(\Omega; \mathbb{R}^2) \rightarrow \mathbf{0}.$$

To provide a more effective explanation of how (15) is derived from (14), we present a step-by-step breakdown of the process. The anti-commutativity $\text{div } \mathbf{v} = 2 \text{sskw}(\text{curl } \mathbf{v})$ is exactly the first identity in (7), by which we can change $\mathbf{H}(\text{div}, \Omega; \mathbb{M})$ to $\mathbf{H}(\text{div}, \Omega; \mathbb{S})$ as follows. For $\mathbf{u} \in \mathbf{L}^2(\Omega; \mathbb{R}^2)$, by the exactness of the bottom complex in (14), there exists $\boldsymbol{\tau} \in \mathbf{H}(\text{div}, \Omega; \mathbb{M})$ satisfying $\mathbf{u} = \text{div } \boldsymbol{\tau}$. Then apply the top complex in (14) to find $\mathbf{v} \in \mathbf{H}^1(\Omega; \mathbb{R}^2)$ satisfying $-2 \text{sskw } \boldsymbol{\tau} = \text{div } \mathbf{v}$. Set $\boldsymbol{\sigma} = \boldsymbol{\tau} + \text{curl } \mathbf{v} \in \mathbf{H}(\text{div}, \Omega; \mathbb{M})$. Clearly $\text{div } \boldsymbol{\sigma} = \text{div } \boldsymbol{\tau} = \mathbf{u}$. By the anti-commutativity, we have $2 \text{sskw } \boldsymbol{\sigma} = 2 \text{sskw } \boldsymbol{\tau} + 2 \text{sskw}(\text{curl } \mathbf{v}) = 2 \text{sskw } \boldsymbol{\tau} + \text{div } \mathbf{v} = 0$, i.e. $\boldsymbol{\sigma} \in \mathbf{H}(\text{div}, \Omega; \mathbb{S})$. This explains the div

stability $\operatorname{div} \mathbf{H}(\operatorname{div}, \Omega; \mathbb{S}) = \mathbf{L}^2(\Omega; \mathbb{R}^2)$. The relation of these functions is summarized below:

$$\begin{array}{ccccc} & & \mathbf{v} & \xrightarrow{\operatorname{div}} & -2 \operatorname{sskw}(\boldsymbol{\tau}) \\ & \swarrow \operatorname{id} & & \nearrow & \\ \mathbf{v} & \xrightarrow{\operatorname{curl}} & \boldsymbol{\tau} & \xrightarrow{\operatorname{div}} & \mathbf{u} \\ & & & \nearrow -2 \operatorname{sskw} & \end{array} .$$

The composition of two curl operators leads to $H^2(\Omega) \xrightarrow{\operatorname{Air}} \mathbf{H}(\operatorname{div}, \Omega; \mathbb{S})$. The null space $\ker(\operatorname{Air})$ consists of $\mathbb{R} + \mathbb{R}^2 \cdot \mathbf{x}^\perp = \mathbb{P}_1$.

The BGG diagram

(16)

$$\begin{array}{ccccccc} \mathbb{R}^2 & \xrightarrow{\subset} & \mathbf{H}^1(\Omega; \mathbb{R}^2) & \xrightarrow{\operatorname{curl}} & \mathbf{H}(\operatorname{divdiv}, \Omega; \mathbb{M}) & \xrightarrow{\operatorname{div}} & \mathbf{H}^{-1,0}(\operatorname{div}, \Omega) \longrightarrow \mathbf{0} \\ & \nearrow & & \nearrow \operatorname{mskw} & & \nearrow \operatorname{id} & \\ \mathbb{R} & \xrightarrow{\subset} & L^2(\Omega) & \xrightarrow{\operatorname{curl}} & \mathbf{H}^{-1,0}(\operatorname{div}, \Omega) & \xrightarrow{\operatorname{div}} & L^2(\Omega) \longrightarrow 0 \end{array}$$

will lead to the divdiv complex

$$\mathbf{RT} \xrightarrow{\subset} \mathbf{H}^1(\Omega; \mathbb{R}^2) \xrightarrow{\operatorname{sym curl}} \mathbf{H}(\operatorname{divdiv}, \Omega; \mathbb{S}) \xrightarrow{\operatorname{divdiv}} L^2(\Omega) \rightarrow 0,$$

and, again by rotation, the strain complex

$$\mathbf{RM} \xrightarrow{\subset} \mathbf{H}^1(\Omega; \mathbb{R}^2) \xrightarrow{\operatorname{sym grad}} \mathbf{H}(\operatorname{rotrot}, \Omega; \mathbb{S}) \xrightarrow{\operatorname{rotrot}} L^2(\Omega) \rightarrow 0,$$

where $\mathbf{RT} := \mathbb{R}^2 + \mathbf{x}\mathbb{R}$ and $\mathbf{RM} := \mathbb{R}^2 + \mathbf{x}^\perp\mathbb{R}$.

The anti-commutativities in (16) are $\operatorname{curl}(c\mathbf{x}) = \operatorname{mskw} c$ for $c \in \mathbb{R}$ and $\operatorname{div}(\operatorname{mskw} v) = -\operatorname{curl} v$ for $v \in L^2(\Omega)$. For $p \in L^2(\Omega)$, by the exactness of the bottom complex in (16), there exists $\mathbf{u} \in \mathbf{H}^{-1,0}(\operatorname{div}, \Omega)$ satisfying $p = \operatorname{div} \mathbf{u}$. Then apply the top complex in (16) to find $\boldsymbol{\tau} \in \mathbf{H}(\operatorname{divdiv}, \Omega; \mathbb{M})$ s.t. $\mathbf{u} = \operatorname{div} \boldsymbol{\tau}$. Set $\boldsymbol{\sigma} = \boldsymbol{\tau} + \operatorname{mskw} w \in \mathbf{H}(\operatorname{divdiv}, \Omega; \mathbb{M})$ with $w = -\operatorname{sskw} \boldsymbol{\tau} \in L^2(\Omega)$. By the anti-community, $\operatorname{div} \operatorname{div}(\operatorname{mskw} w) = -\operatorname{div}(\operatorname{curl} w) = 0$. Hence $\operatorname{div} \operatorname{div} \boldsymbol{\sigma} = \operatorname{div} \operatorname{div} \boldsymbol{\tau} = p$, and $\operatorname{sskw} \boldsymbol{\sigma} = \operatorname{sskw} \boldsymbol{\tau} + \operatorname{sskw}(\operatorname{mskw} w) = \operatorname{sskw} \boldsymbol{\tau} + w = 0$, i.e. $\boldsymbol{\sigma} \in \mathbf{H}(\operatorname{divdiv}, \Omega; \mathbb{S})$. This explains $\operatorname{div} \operatorname{div} \mathbf{H}(\operatorname{divdiv}, \Omega; \mathbb{S}) = L^2(\Omega)$. The chase of the diagram is summarized below:

$$\begin{array}{ccccc} & & \boldsymbol{\tau} & \xrightarrow{\operatorname{div}} & \mathbf{u} \\ & \nearrow -\operatorname{sskw} & & \nearrow \operatorname{id} & \\ w & \xrightarrow{\operatorname{curl}} & \mathbf{u} & \xrightarrow{\operatorname{div}} & p \end{array} .$$

The null space $\ker(\operatorname{sym curl})$ is given by $\mathbb{R}^2 + \mathbf{x}\mathbb{R} = \mathbf{RT}$.

We shall construct finite element counterparts of the BGG diagrams (14)-(16), and derive several finite element elasticity and divdiv complexes. The first step is to design finite element de Rham complexes of different smoothness.

3. SMOOTH FINITE ELEMENTS IN TWO DIMENSIONS

In this section, we shall construct C^m -continuous finite elements on two-dimensional triangular grids, firstly constructed by Bramble and Zlámal [10], by a decomposition of the simplicial lattice.

We use a pair of integers $\mathbf{r} = (r^v, r^e)$ for the smoothness at vertices and at edges, respectively. Value -1 means no continuity. To be C^m -continuous, $r^e = m$ is the minimum requirement for edges and $r^v \geq \max\{2r^e, -1\}$ for vertices. The polynomial degree $k \geq \max\{2r^v + 1, 0\}$. For a vector $\mathbf{r} \in \mathbb{R}^d$ and a constant c , $\mathbf{r} \geq c$ means $r_i \geq c$

for all components $i = 1, 2, \dots, d$, and $\mathbf{r} + \mathbf{c} := (r_1 + c, r_2 + c, \dots, r_d + c)$. Define $\mathbf{r} \ominus 1 := \max\{\mathbf{r} - 1, -1\}$

3.1. Simplicial lattice. For two non-negative integers $l \leq m$, we will use the multi-index notation $\alpha \in \mathbb{N}^{l:m}$, meaning $\alpha = (\alpha_l, \dots, \alpha_m)$ with integer $\alpha_i \geq 0$. The length of α is $m - l + 1$. The sum (absolute value) of a multi-index is $|\alpha| := \sum_{i=l}^m \alpha_i$ for $\alpha \in \mathbb{N}^{l:m}$ and the factorial is $\alpha! := \alpha_l! \cdots \alpha_m!$. Denote

$$D^\beta := \frac{\partial^{|\beta|}}{\partial x_1^{\beta_1} \partial x_2^{\beta_2}}, \quad \beta \in \mathbb{N}^{1:2}.$$

A simplicial lattice of degree $k \geq 1$ in two dimensions is a multi-index set of length 3 with fixed sum k , i.e.,

$$\mathbb{T}_k^2 := \{\alpha = (\alpha_0, \alpha_1, \alpha_2) \in \mathbb{N}^{0:2} \mid |\alpha| = k\}.$$

An element $\alpha \in \mathbb{T}_k^2$ is called a node of the lattice.

We can embed the simplicial lattice \mathbb{T}_k^2 into a triangle T with vertices $\{v_0, v_1, v_2\}$. Given $\alpha \in \mathbb{T}_k^2$, the barycentric coordinate of α is given by $\lambda(\alpha) = (\alpha_0, \alpha_1, \alpha_2)/k$, and the geometric embedding is

$$x : \mathbb{T}_k^2 \rightarrow T, \quad x(\alpha) = \sum_{i=0}^2 \lambda_i(\alpha) v_i.$$

The left side of Fig. 1 illustrates the embedding of a two-dimensional simplicial lattice \mathbb{T}_8^2 within a reference triangle \hat{T} with vertices $(0, 0), (1, 0), (0, 1)$, while the right side shows the embedding of the same lattice into an equilateral triangle.

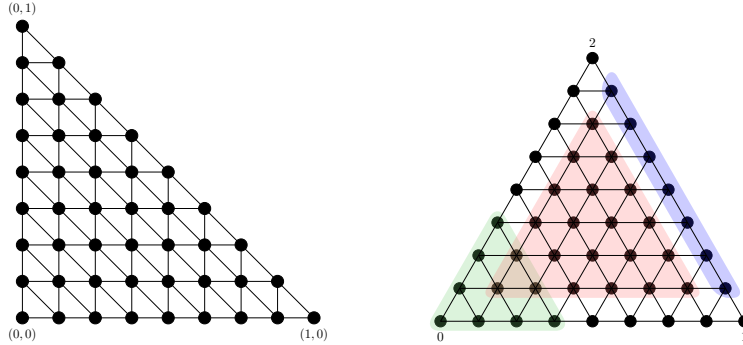


FIGURE 1. Two embeddings of the simplicial lattice \mathbb{T}_8^2 in two dimensions.

A simplicial lattice \mathbb{T}_k^2 is, by definition, an algebraic set. Through the geometric embedding $\mathbb{T}_k^2(T)$, we can apply operators for the geometric simplex T . For example, for a subset $S \subseteq T$, we use $\mathbb{T}_k^2(S) = \{\alpha \in \mathbb{T}_k^2, x(\alpha) \in S\}$ to denote the portion of lattice nodes whose geometric embedding is inside S .

3.2. Bernstein basis. It holds that

$$|\mathbb{T}_k^2| = \binom{k+2}{k} = \dim \mathbb{P}_k(T).$$

Let T be a triangle with vertices $\{v_0, v_1, v_2\}$ and $\lambda_i, i = 0, 1, 2$, be the barycentric coordinate. The Bernstein basis of $\mathbb{P}_k(T)$ is

$$\{\lambda^\alpha := \lambda_0^{\alpha_0} \lambda_1^{\alpha_1} \lambda_2^{\alpha_2} \mid \alpha \in \mathbb{T}_k^2\}.$$

For a subset $S \subseteq \mathbb{T}_k^2$, we define

$$\mathbb{P}_k(S) := \text{span}\{\lambda^\alpha, \alpha \in S \subseteq \mathbb{T}_k^2\}.$$

By establishing a one-to-one mapping between the lattice node α and the corresponding Bernstein polynomial λ^α , we can analyze polynomial properties through the simplicial lattice. In fact, all lattice nodes serve as interpolation nodes for the k -th order Lagrange element.

3.3. Sub-simplicial lattices and distance. We adopt the notation of [6] and define $\Delta(T)$ as the set of all sub-simplices of T , and $\Delta_\ell(T)$ as the set of all sub-simplices of dimension ℓ , where $0 \leq \ell \leq 2$. A sub-simplex $f \in \Delta_\ell(T)$ is determined by choosing $\ell + 1$ vertices from the 3 vertices of T . We will overload the notation f for both the geometric simplex and the algebraic set of indices. As an algebraic set, $f = \{f(0), \dots, f(\ell)\} \subseteq \{0, 1, 2\}$ is a subset of indices, and also

$$f = \text{Convex}(v_{f(0)}, \dots, v_{f(\ell)}) \in \Delta_\ell(T)$$

is the ℓ -dimensional simplex spanned by the vertices $v_{f(0)}, \dots, v_{f(\ell)}$. We also use notation e_{ij} for the edge formed by vertices v_i and v_j for $i, j = 0, 1, 2, i \neq j$.

For $\ell = 0, 1$ and $f \in \Delta_\ell(T)$, we let $f^* \in \Delta_{2-\ell-1}(T)$ denote the sub-simplex of T opposite to f . When treating f as a subset of $\{0, 1, 2\}$, $f^* \subset \{0, 1, 2\}$ so that $f \cup f^* = \{0, 1, 2\}$, i.e., f^* is the complementary set of f . Geometrically,

$$f^* = \text{Convex}(v_{f^*(1)}, \dots, v_{f^*(2-\ell)}) \in \Delta_{1-\ell}(T)$$

represents the $(1 - \ell)$ -dimensional simplex spanned by vertices not contained in f . When f is a vertex v_i , we simply write f^* as i^* . Note that f can be identified as the zero level set of the barycentric coordinate associated with the index set f^* , i.e., $f = \{x \in T \mid \lambda_i(x) = 0, \text{ for all } i \in f^*\}$.

Given a sub-simplex $f \in \Delta_\ell(T)$, through the geometric embedding $f \hookrightarrow T$, we define the prolongation/extension operator $E_f : \mathbb{T}_k^\ell(f) \rightarrow \mathbb{T}_k^2(T)$ as follows:

$$E_f(\alpha)_{f(i)} = \alpha_i, i = 0, \dots, \ell, \quad \text{and } E_f(\alpha)_j = 0, j \notin f.$$

For example, for $\alpha = (\alpha_0, \alpha_1) \in \mathbb{T}_k^1(f)$, when $f = \{1, 2\}$, the extension $E_f(\alpha) = (0, \alpha_0, \alpha_1) \in \mathbb{T}_k^2(T)$, and when $f = \{0, 2\}$, the extension $E_f(\alpha) = (\alpha_0, 0, \alpha_1) \in \mathbb{T}_k^2(T)$. The geometric embedding $x(E_f(\alpha)) \in f$ justifies the notation $\mathbb{T}_k^\ell(f)$. With a slight abuse of notation, for a node $\alpha_f \in \mathbb{T}_k^\ell(f)$, we still use the same notation $\alpha_f \in \mathbb{T}_k^2(T)$ to denote $E_f(\alpha_f)$. Then we have the following direct decomposition

$$(17) \quad \alpha = E_f(\alpha_f) + E_{f^*}(\alpha_{f^*}) = \alpha_f + \alpha_{f^*}, \text{ and } |\alpha| = |\alpha_f| + |\alpha_{f^*}|.$$

Based on (17), we can write a Bernstein polynomial as

$$\lambda^\alpha = \lambda_f^{\alpha_f} \lambda_{f^*}^{\alpha_{f^*}},$$

where $\lambda_f = \lambda_{f(0)} \dots \lambda_{f(\ell)} \in \mathbb{P}_{\ell+1}(f)$ is the bubble function on f and also denoted by b_f .

The bubble polynomial of f is

$$b_f \mathbb{P}_{k-(\ell+1)}(f) := \text{span}\{b_f \lambda_f^{\alpha_f} : \alpha_f \in \mathbb{T}_{k-(\ell+1)}^\ell(f)\}.$$

Geometrically as the bubble polynomial space vanished on the boundary, it is generated by the interior lattice nodes only. In Fig. 1, $\mathbb{T}_k^2(\overset{\circ}{T})$ consists of the nodes inside the red triangle, and $\mathbb{T}_k^1(\overset{\circ}{f})$ for $f = \{1, 2\}$ is in the blue trapezoid region.

3.4. Derivative and distance. Given $f \in \Delta_\ell(T)$, we define the distance of a node $\alpha \in \mathbb{T}_k^2$ to f as

$$\text{dist}(\alpha, f) := |\alpha_{f^*}| = \sum_{i \in f^*} \alpha_i.$$

We define the lattice tube of f with radius r as

$$D(f, r) := \{\alpha \in \mathbb{T}_k^2, \text{dist}(\alpha, f) \leq r\},$$

which contains lattice nodes at most r distance away from f . Define

$$L(f, s) := \{\alpha \in \mathbb{T}_k^2, \text{dist}(\alpha, f) = s\}.$$

Then by definition,

$$D(f, r) = \cup_{s=0}^r L(f, s), \quad L(f, s) = L(f^*, k - s).$$

We have the following characterization of lattice nodes in $D(f, r)$.

Lemma 3.1. *For lattice node $\alpha \in \mathbb{T}_k^2$,*

$$\begin{aligned} \alpha \in D(f, r) &\iff |\alpha_{f^*}| \leq r \iff |\alpha_f| \geq k - r, \\ \alpha \notin D(f, r) &\iff |\alpha_{f^*}| > r \iff |\alpha_f| \leq k - r - 1. \end{aligned}$$

Proof. By definition of $\text{dist}(\alpha, f)$ and the fact $|\alpha_f| + |\alpha_{f^*}| = k$. □

For each vertex $v_i \in \Delta_0(T)$ and an integer $0 \leq r \leq k$, the tube

$$D(v_i, r) = \{\alpha \in \mathbb{T}_k^2(T), |\alpha_{i^*}| \leq r\},$$

is isomorphic to a simplicial lattice \mathbb{T}_r^2 of degree r . In Fig. 1, $D(v_0, 3)$ consists of lattice nodes in the green triangle which itself can be treated as a smaller simplicial lattice \mathbb{T}_3^2 . For an edge $e \in \Delta_1(T)$, $D(e, r)$ is a trapezoid of height r with base e .

Recall that in [6] a smooth function u is said to vanish to order r on f if $D^\beta u|_f = 0$ for all $\beta \in \mathbb{N}^{1:2}$ satisfying $|\beta| < r$. The following result shows that the vanishing order r of a Bernstein polynomial λ^α on a sub-simplex f is the distance $\text{dist}(\alpha, f)$.

Lemma 3.2. *Let $f \in \Delta_\ell(T)$ be a sub-simplex of T . For $\alpha \in \mathbb{T}_k^2$, $\beta \in \mathbb{N}^{1:2}$, and $|\alpha_{f^*}| > |\beta|$, i.e., $\text{dist}(\alpha, f) > |\beta|$, then*

$$D^\beta \lambda^\alpha|_f = 0, \quad \text{when } \text{dist}(\alpha, f) > |\beta|.$$

Proof. For $\alpha \in \mathbb{T}_k^2$, we write $\lambda^\alpha = \lambda_f^{\alpha_f} \lambda_{f^*}^{\alpha_{f^*}}$. When $|\alpha_{f^*}| > |\beta|$, the derivative $D^\beta \lambda^\alpha$ will contain a factor $\lambda_{f^*}^\gamma$ with $\gamma \in \mathbb{N}^{1:(2-\ell)}$, and $|\gamma| = |\alpha_{f^*}| - |\beta| > 0$. Therefore $D^\beta \lambda^\alpha|_f = 0$ as $\lambda_i|_f = 0$ for $i \in f^*$. □

3.5. Derivatives at vertices. Consider a function $u \in C^m(\Omega)$. The set of derivatives of order up to m can be written as

$$\{D^\beta u, \beta \in \mathbb{N}^{1:2}, |\beta| \leq m\}.$$

Notice that the multi-index $\beta \in \mathbb{N}^{1:2}$ is not in $\mathbb{N}^{0:2}$. We can add a component with value $m - |\beta|$ to form a simplicial lattice \mathbb{T}_m^2 of degree m , which can be used to determine the derivatives at that vertex.

Lemma 3.3. *Let $i \in \{0, 1, 2\}$. The polynomial space*

$$\mathbb{P}_k(D(v_i, m)) := \text{span} \left\{ \lambda^\alpha, \alpha \in \mathbb{T}_k^2, \text{dist}(\alpha, v_i) = |\alpha_{i^*}| \leq m \right\},$$

is uniquely determined by the DoFs

$$(18) \quad \{D^\beta u(v_i), \beta \in \mathbb{N}^{1:2}, |\beta| \leq m\}.$$

Proof. Without loss of generality, consider v_0 . Define map $\alpha = (\alpha_0, \alpha_1, \alpha_2) \rightarrow \beta = (\alpha_1, \alpha_2)$ which induces a one-to-one map from $D(v_0, m) = \{\alpha \in \mathbb{T}_k^2, \alpha_1 + \alpha_2 \leq m\}$ to $\{\beta \in \mathbb{N}^{1:2}, |\beta| \leq m\}$. So the dimension of $\mathbb{P}_k(D(v_i, m))$ matches the number of DoFs (18). It suffices to show that for $u \in \mathbb{P}_k(D(v_0, m))$ if DoFs (18) vanish, then $u = 0$.

Recall the multivariate calculus result

$$(19) \quad D^\beta(x_1^{\alpha_1} x_2^{\alpha_2}) = \beta! \delta(\alpha, \beta) \text{ for } \alpha, \beta \in \mathbb{N}^{1:2}, |\alpha| = |\beta| = r \geq 0,$$

where $\delta(\alpha, \beta)$ is the Kronecker delta function. When the triangle T is the reference triangle, v_0 is the origin and $\lambda_1 = x_1, \lambda_2 = x_2$. So we conclude that the homogenous polynomial space $\text{span} \{x_1^{\alpha_1} x_2^{\alpha_2}, \alpha \in \mathbb{N}^{1:2}, |\alpha| = r\}$ is determined by DoFs $\{D^\beta u(v_0), \beta \in \mathbb{N}^{1:2}, |\beta| = r\}$. Running $r = 0, 1, \dots, m$, we then finish the proof when the triangle is the reference triangle.

For a general triangle, instead of changing to the reference triangle, we shall use the barycentric coordinate. Clearly $\{\nabla \lambda_1, \nabla \lambda_2\}$ forms a basis of \mathbb{R}^2 . Choose another basis $\{l^1, l^2\}$ of \mathbb{R}^2 , being dual to $\{\nabla \lambda_1, \nabla \lambda_2\}$, i.e., $\nabla \lambda_i \cdot l^j = \delta_{i,j}$ for $i, j = 1, 2$. Indeed l^i is the edge vector e_{0i} as $\nabla \lambda_i$ is orthogonal to e_{0i} for $i = 1, 2$. We can express the derivatives in this non-orthogonal basis and denote by $D_n^\beta u := \frac{\partial^{|\beta|} u}{\partial (l^1)^{\beta_1} \partial (l^2)^{\beta_2}}$ with $\frac{\partial}{\partial l^i} = l^i \cdot \nabla$. By the duality $\nabla \lambda_i \cdot l^j = \delta_{i,j}$, $i, j = 1, 2$, we have the generalization of (19)

$$(20) \quad D_n^\beta(\lambda_1^{\alpha_1} \lambda_2^{\alpha_2}) = \beta! \delta(\alpha, \beta) \quad \text{for } \alpha, \beta \in \mathbb{N}^{1:2}, |\alpha| = |\beta| = r.$$

By the chain rule, it is easy to show that the vanishing $\{D_n^\beta u, \beta \in \mathbb{N}^{1:2}, |\beta| \leq m\}$ is equivalent to the vanishing $\{D^\beta u, \beta \in \mathbb{N}^{1:2}, |\beta| \leq m\}$. So we will work with D_n^β .

A Bernstein basis of $\mathbb{P}_k(D(v_0, m))$ is given by $\{\lambda_0^{k-|\alpha|} \lambda_1^{\alpha_1} \lambda_2^{\alpha_2}, \alpha \in \mathbb{N}^{1:2}, |\alpha| \leq m\}$. Assume $u = \sum_{\substack{\alpha \in \mathbb{N}^{1:2} \\ |\alpha| \leq m}} c_\alpha \lambda_0^{k-|\alpha|} \lambda_1^{\alpha_1} \lambda_2^{\alpha_2}$ with $c_\alpha \in \mathbb{R}$ and $D^\beta u(v_0) = 0$ for all $\beta \in \mathbb{N}^{1:2}$ satisfying $|\beta| \leq m$. We shall prove $c_\alpha = 0$ by induction.

For $|\alpha| = 0$, as $c_{(0,0)} = u(v_0) = 0$, we conclude $c_{(0,0)} = 0$. Assume $c_\alpha = 0$ for all $\alpha \in \mathbb{N}^{1:2}$ satisfying $|\alpha| \leq r-1$, i.e., $u = \sum_{\substack{\alpha \in \mathbb{N}^{1:2} \\ r \leq |\alpha| \leq m}} c_\alpha \lambda_0^{k-|\alpha|} \lambda_1^{\alpha_1} \lambda_2^{\alpha_2}$. By Lemma 3.2, the derivative $D^\beta(\lambda_0^{k-|\alpha|} \lambda_1^{\alpha_1} \lambda_2^{\alpha_2})$ vanishes at v_0 for all $\beta \in \mathbb{N}^{1:2}$ satisfying $|\beta| < |\alpha|$. Hence, for $|\beta| = r$, using (20),

$$D_n^\beta u(v_0) = D_n^\beta \left(\sum_{\alpha \in \mathbb{N}^{1:2}, |\alpha|=r} c_\alpha \lambda_0^{k-r} \lambda_1^{\alpha_1} \lambda_2^{\alpha_2} \right) (v_0) = \beta! c_\beta = 0,$$

which implies $c_\beta = 0$ for all $\beta \in \mathbb{N}^{1:2}, |\beta| = r$. Running $r = 1, 2, \dots, m$, we conclude $u = 0$. \square

3.6. Normal derivatives on edges. Given an edge e , we identify lattice nodes to determine the normal derivative up to order m

$$\left\{ \frac{\partial^\beta u}{\partial n_e^\beta} \Big|_e, 0 \leq \beta \leq m \right\}.$$

By Lemma 3.2, if the lattice node is $r^e + 1$ away from the edge, then the corresponding Bernstein polynomial will have vanishing normal derivatives up to order r^e .

We have used lattice nodes $D(\Delta_0(e), r^v) := \cup_{v \in \Delta_0(e)} D(v, r^v)$ to determine the derivatives at vertices. We will use $D(e, r^e) \setminus D(\Delta_0(e), r^v)$ for the normal derivative.

Lemma 3.4. *Let $r^v \geq r^e \geq 0$ and $k \geq 2r^v + 1$. Let $e \in \Delta_1(T)$ be an edge of a triangle T . The polynomial function space $\mathbb{P}_k(D(e, r^e) \setminus D(\Delta_0(e), r^v))$ is determined by DoFs*

$$\int_e \frac{\partial^\beta u}{\partial n_e^\beta} \lambda_e^\alpha ds \quad \alpha \in \mathbb{T}_{k-2(r^v+1)+\beta}^1, \beta = 0, 1, \dots, r^e.$$

Proof. Without loss of generality, take $e = e_{0,1}$. By definition $D(e, r^e) = \cup_{i=0}^{r^e} L(e, i)$, where recall that

$$L(e, i) = \{\alpha \in \mathbb{T}_k^2, \text{dist}(\alpha, e) = i\} = \{\alpha \in \mathbb{T}_k^2, \alpha_0 + \alpha_1 = k - i\}$$

consists of lattice nodes parallel to e and with distance i . Define the map $(\alpha_0, \alpha_1, \alpha_2) \rightarrow (\alpha_0, \alpha_1)$ which is one-to-one between $L(e, i)$ and $\mathbb{T}_{k-i}^1(e)$.

Now we use the requirement $\alpha \notin D(\Delta_0(e), r^v)$ to figure out the bound of the components. Using Lemma 3.1, we derive from $\text{dist}(\alpha, v_0) > r^v$ that $\alpha_0 < k - r^v$. Together with $\alpha_0 + \alpha_1 = k - i$, we get the lower bound $\alpha_1 \geq r^v - i + 1$. Similarly $\alpha_0 \geq r^v - i + 1$. Therefore

$$L(e, i) \setminus D(\Delta_0(e), r^v) = \{(\alpha_0, \alpha_1, i), \alpha_0 + \alpha_1 = k - i, \min\{\alpha_0, \alpha_1\} \geq r^v - i + 1\}.$$

Define the one-to-one mapping

$$\begin{aligned} \mathbb{T}_{k-2(r^v+1)+i}^1 &\rightarrow L(e, i) \setminus D(\Delta_0(e), r^v), \\ (\alpha_0, \alpha_1) &\mapsto (\alpha_0 + (r^v - i + 1), \alpha_1 + (r^v - i + 1), i). \end{aligned}$$

With the help of this one-to-one mapping, we shall prove the polynomial function space $\mathbb{P}_k(L(e, i) \setminus D(\Delta_0(e), r^v))$ is determined by DoFs

$$(21) \quad \int_e \frac{\partial^i u}{\partial n_e^i} \lambda_e^\alpha ds \quad \alpha \in \mathbb{T}_{k-2(r^v+1)+i}^1.$$

Take a $u = \sum_{\alpha \in \mathbb{T}_{k-2(r^v+1)+i}^1} c_\alpha \lambda_e^{\alpha+r^v-i+1} \lambda_2^i \in \mathbb{P}_k(L(e, i) \setminus D(\Delta_0(e), r^v))$ with coefficients $c_\alpha \in \mathbb{R}$. By the chain rule and the fact $\lambda_2|_e = 0$, in the non-zero terms of $\frac{\partial^i u}{\partial n_e^i}|_e$, the derivative in $\frac{\partial^i u}{\partial n_e^i}|_e$ will all apply to λ_2^i , so

$$\frac{\partial^i u}{\partial n_e^i}|_e = i!(n_e \cdot \nabla \lambda_2)^i \lambda_e^{r^v-i+1} \sum_{\alpha \in \mathbb{T}_{k-2(r^v+1)+i}^1} c_\alpha \lambda_e^\alpha|_e.$$

Noting that $n_e \cdot \nabla \lambda_2$ is a constant and the bubble polynomial $\lambda_e^{r^v-i+1}$ is always positive in the interior of e , the vanishing DoF (21) means $c_\alpha = 0$ for all $\alpha \in \mathbb{T}_{k-2(r^v+1)+i}^1$.

It follows from Lemma 3.2 that $\frac{\partial^\beta}{\partial n_e^\beta}(\lambda_e^\alpha \lambda_2^i)|_e = 0$ for $\alpha \in \mathbb{T}_{k-i}^1(e)$ and $0 \leq \beta < i \leq r^e$. That is the matrix

$$\left(\frac{\partial^\beta}{\partial n_e^\beta}(\lambda_e^\alpha \lambda_2^i)|_e \right)_{0 \leq \beta \leq r^e, 0 \leq i \leq r^e, \alpha \in \mathbb{T}_{k-2(r^v+1)+i}^1(e)}$$

is lower block triangular as follows.

$$\begin{array}{c}
\beta \setminus i \\
\alpha \\
0 \\
1 \\
\vdots \\
r^e - 1 \\
r^e
\end{array}
\begin{array}{c}
0 \quad 1 \quad \dots \quad r^e - 1 \quad r^e \\
\mathbb{T}_{k-2(r^v+1)}^1 \quad \mathbb{T}_{k-2(r^v+1)+1}^1 \quad \dots \quad \mathbb{T}_{k-2(r^v+1)+r^e-1}^1 \quad \mathbb{T}_{k-2(r^v+1)+r^e}^1 \\
\left(\begin{array}{c|c|c|c|c}
\Box & 0 & \dots & 0 & 0 \\
\Box & \Box & \dots & 0 & 0 \\
\vdots & \vdots & \ddots & \vdots & \vdots \\
\Box & \Box & \dots & \Box & 0 \\
\Box & \Box & \dots & \Box & \Box
\end{array} \right)
\end{array}$$

Since we have proved each block matrix is invertible, then the whole lower block triangular matrix is invertible which is equivalent to the unisolvence. \square

3.7. Geometric decompositions of the simplicial lattice. Inside a triangle, a vertex will be shared by two edges and to have enough lattice nodes for each edge, $r^v \geq 2r^e$ is required; see Fig. 2(b).

Lemma 3.5. *Let $r^e = m \geq -1$, $r^v \geq \max\{2r^e, -1\}$, and nonnegative integer $k \geq 2r^v + 1 \geq 4m + 1$. Let T be a triangle. Then it holds that*

$$(22) \quad \mathbb{T}_k^2(T) = S_0(T) \oplus S_1(T) \oplus S_2(T),$$

where

$$\begin{aligned}
S_0(T) &:= D(\Delta_0(T), r^v), \\
S_1(T) &:= \bigoplus_{e \in \Delta_1(T)} (D(e, r^e) \setminus S_0(T)), \\
S_2(T) &:= \mathbb{T}_k^2(T) \setminus (S_0(T) \oplus S_1(T)),
\end{aligned}$$

with cardinality

$$\begin{aligned}
|S_0(T)| &= 3 \binom{r^v + 2}{2}, \\
|S_1(T)| &= 3 \sum_{i=0}^{r^e} (k - 1 - 2r^v + i), \\
|S_2(T)| &= \binom{k + 2}{2} - |S_0(T)| - |S_1(T)|.
\end{aligned}$$

This leads to the decomposition of the polynomial space

$$(23) \quad \mathbb{P}_k(T) = \mathbb{P}_k(S_0(T)) \oplus \mathbb{P}_k(S_1(T)) \oplus \mathbb{P}_k(S_2(T)).$$

Proof. As $k \geq 2r^v + 1$, the sets $\{D(v, r^v), v \in \Delta_0(T)\}$ are disjoint.

We then show that the sets $\{D(e, r^e) \setminus D(\Delta_0(e), r^v), e \in \Delta_1(T)\}$ are disjoint. A node $\alpha \in D(e_{01}, r^e)$ implies $\alpha_2 \leq r^e$ and $\alpha \in D(e_{02}, r^e)$ implies $\alpha_1 \leq r^e$. Therefore $|\alpha_{0*}| = \alpha_1 + \alpha_2 \leq 2r^e \leq r^v$, i.e., $D(e_{01}, r^e) \cap D(e_{02}, r^e) \subseteq D(v_0, r^v)$. Repeat the argument for each pair of edges to conclude $\{D(e, r^e) \setminus D(\Delta_0(e), r^v), e \in \Delta_1(T)\}$ are disjoint.

For a given edge e , the vertex e^* is opposite to e and $L(e^*, r^v) = L(e, k - r^v)$. As $k - r^v \geq r^v + 1 > r^e$, we conclude $D(e, r^e) \cap D(e^*, r^v) = \emptyset$ and consequently $D(e, r^e) \setminus D(\Delta_0(T), r^v) = D(e, r^e) \setminus D(\Delta_0(e), r^v)$.

Then decompositions (22) and (23) follow. \square

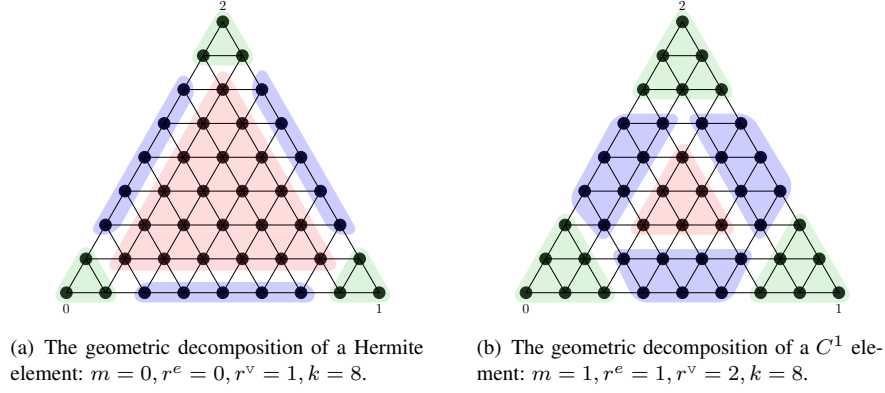


FIGURE 2. Comparison of the geometric decompositions of a two-dimensional Hermite element and a C^1 -conforming element.

Denote by

$$\mathbb{B}_k(\mathbf{r}) = \mathbb{B}_k(\mathbf{r}; T) := \mathbb{P}_k(S_2(T)) = \text{span}\{\lambda^\alpha, \alpha \in S_2(T)\},$$

and call it the polynomial bubble space, which will play an important role in our construction of finite element de Rham complexes. Polynomials in $\mathbb{B}_k(\mathbf{r})$ will have vanishing derivatives up to order r^e , and more precisely

$$\mathbb{B}_k(\mathbf{r}, T) = \{u \in \mathbb{P}_k(T) : \nabla^j u \text{ vanishes at all vertices of } T \text{ for } j = 0, \dots, r^v, \\ \text{and } \nabla^j u \text{ vanishes on all edges of } T \text{ for } j = 0, \dots, r^e\}.$$

Lemma 3.6. *Let $r^e \geq -1$ and $r^v \geq \max\{2r^e, -1\}$. Then*

- (1) $\dim \mathbb{B}_k(\mathbf{r}) \geq 1$, when $k \geq \max\{2r^v + 1, 3r^e + 3, (r^e + 3)[r^v = 0]\}$;
- (2) $\dim \mathbb{B}_k(\mathbf{r}) \geq 3$, when $k \geq \max\{2r^v + 1, 3r^e + 4, 4[r^e = -1, r^v = 1], 2[r^e = -1, r^v = 0]\}$.

Proof. The first statement has been proved in [14]. We can prove the second statement by verifying the following inequality directly

$$\dim \mathbb{B}_k(\mathbf{r}) = \binom{k - 3r^e - 1}{2} - 3 \binom{r^v - 2r^e}{2} \geq 3.$$

□

3.8. Smooth finite elements in two dimensions. We are in the position to present C^m -finite elements on a triangulation.

Theorem 3.7. *Let $r^e = m \geq -1$, $r^v \geq \max\{2r^e, -1\}$, and nonnegative integer $k \geq 2r^v + 1$. Let T be a triangle. The shape function space $\mathbb{P}_k(T)$ is determined by the DoFs*

$$(24a) \quad D^\alpha u(v) \quad \alpha \in \mathbb{N}^{1:2}, |\alpha| \leq r^v, v \in \Delta_0(T),$$

$$(24b) \quad \int_e \frac{\partial^\beta u}{\partial n_e^\beta} q \, ds \quad q \in \mathbb{P}_{k-2(r^v+1)+\beta}(e), \beta = 0, \dots, r^e, e \in \Delta_1(T),$$

$$(24c) \quad \int_T u q \, dx \quad q \in \mathbb{B}_k(\mathbf{r}).$$

Proof. By the decomposition (23) of $\mathbb{P}_k(T)$, the dimension of $\mathbb{P}_k(T)$ matches the number of DoFs. Let $u \in \mathbb{P}_k(T)$ satisfy all the DoFs (24a)-(24c) vanish. Thanks to Lemma 3.3, Lemma 3.4 and Lemma 3.5, it follows from the vanishing DoFs (24a) and (24b) that $u \in \mathbb{P}_k(S_2(T))$. Then $u = 0$ holds from the vanishing DoF (24c). \square

When $r^e = m = 1$ and $r^v = 2$, this is known as Argyris element [1, 34]. When $r^e = m, r^v = 2m$ and $k = 4m + 1$, C^m -continuous finite elements have been constructed in [10, 35], see also [31, Section 8.1] and the references therein, whose DoFs are different from (24b)-(24c). Here DoFs (24a)-(24c) are firstly constructed in [28]. The DoFs in [31], also called nodal minimal determining sets in the spline literature, are the point evaluation of functions and their derivatives at some nodes. While DoFs (24b)-(24c) are in the integral form, which is beneficial to the unisolvence of the DoFs and the construction of the finite element de Rham complexes. Smooth finite elements with the DoFs in the integral form on simplexes in arbitrary dimension were firstly constructed in [28].

With mesh \mathcal{T}_h , define the global C^m -continuous finite element space

$$V(\mathcal{T}_h) = \{u \in L^2(\Omega) : u|_T \in \mathbb{P}_k(T) \text{ for all } T \in \mathcal{T}_h, \\ \text{and all the DoFs (24a) and (24b) are single-valued}\}.$$

Since $r^v \geq r^e$, the single-valued DoFs (24a) and (24b) will imply $u \in C^m(\Omega)$.

The finite element space $V(\mathcal{T}_h)$ admits the following geometric decomposition

$$V(\mathcal{T}_h) = \bigoplus_{v \in \Delta_0(\mathcal{T}_h)} \mathbb{P}_k(D(v, r^v)) \oplus \bigoplus_{e \in \Delta_1(\mathcal{T}_h)} \mathbb{P}_k(D(e, r^e) \setminus D(\Delta_0(e), r^v)) \\ \oplus \bigoplus_{T \in \mathcal{T}_h} \mathbb{B}_k(\mathbf{r}, T).$$

The dimension of $V(\mathcal{T}_h)$ is

$$\dim V(\mathcal{T}_h) = |\Delta_0(\mathcal{T}_h)| \binom{r^v + 2}{2} + |\Delta_1(\mathcal{T}_h)| \left[\binom{k - 2r^v + r^e}{2} - \binom{k - 2r^v - 1}{2} \right] \\ + |\Delta_2(\mathcal{T}_h)| \left[\binom{k - 3r^e - 1}{2} - 3 \binom{r^v - 2r^e}{2} \right].$$

In particular, denote by $V^{\text{BZ}}(\mathcal{T}_h)$ the minimum degree case: $r^e = m, r^v = 2m, k = 4m + 1$ with $m \geq 0$, which is firstly constructed in [10], and the dimension is

$$\dim V^{\text{BZ}}(\mathcal{T}_h) = |\Delta_0(\mathcal{T}_h)| \binom{2m + 2}{2} + |\Delta_1(\mathcal{T}_h)| \binom{m + 1}{2} + |\Delta_2(\mathcal{T}_h)| \binom{m}{2}.$$

When $m = 0, 1$, there is no interior moments as $k = 4m + 1$ is not large enough.

4. FINITE ELEMENT DE RHAM COMPLEXES

In this section we shall construct finite element spaces with appropriate DoFs which make the global finite element complexes (25) exact

$$(25) \quad \mathbb{R} \xrightarrow{\subset} \mathbb{V}_{k+1}^{\text{curl}}(\mathcal{T}_h; \mathbf{r}_0) \xrightarrow{\text{curl}} \mathbb{V}_k^{\text{div}}(\mathcal{T}_h; \mathbf{r}_1, \mathbf{r}_2) \xrightarrow{\text{div}} \mathbb{V}_{k-1}^{L^2}(\mathcal{T}_h; \mathbf{r}_2) \rightarrow 0.$$

Space $\mathbb{V}_k(\mathcal{T}_h; \mathbf{r}_2)$ is denoted as $\mathbb{V}_k^{L^2}(\mathcal{T}_h; \mathbf{r}_2)$ to emphasize it is considered as a subspace of $L^2(\Omega)$ although it might be continuous when $\mathbf{r}_2 \geq 0$.

Unlike the classical FEEC [5], additional smoothness on lower sub-simplexes (vertices and edges for a two-dimensional triangulation) will be imposed, which are described by three vectors $\mathbf{r}_0, \mathbf{r}_1$, and \mathbf{r}_2 with the subscript referring to the i -form for $i = 0, 1, 2$. Each $\mathbf{r}_i = (r_i^v, r_i^e)$ consists of two parameters for the smoothness at vertices and edges, respectively, and $r_i^v \geq 2r_i^e$ for $i = 0, 1, 2$. The finite element de Rham complexes constructed

in [28] are exactly complex (25) with $\mathbf{r}_0 = \mathbf{r}_1 + 1$ and $\mathbf{r}_2 = \mathbf{r}_1 - 1$. We shall consider the general case $\mathbf{r}_0 = \mathbf{r}_1 + 1$, $\mathbf{r}_1 \geq -1$, and $\mathbf{r}_2 \geq \mathbf{r}_1 \ominus 1 = \max\{\mathbf{r}_1 - 1, -1\}$.

4.1. Continuous vector finite element space and decay smoothness. We first consider a simple case in which the smoothness parameters are decreased by 1:

$$\mathbf{r}_1 \geq 0, \quad \mathbf{r}_0 = \mathbf{r}_1 + 1, \quad \mathbf{r}_2 = \mathbf{r}_1 - 1.$$

As $\mathbf{r}_1 \geq 0$, $\mathbb{V}_k^{\text{div}}(\mathcal{T}_h; \mathbf{r}_1) = \mathbb{V}_k^2(\mathcal{T}_h; \mathbf{r}_1)$, and $\mathbb{V}_{k+1}^{\text{curl}}(\mathcal{T}_h; \mathbf{r}_0) = \mathbb{V}_{k+1}(\mathcal{T}_h; \mathbf{r}_1)$ is at least in C^1 . In this case, (25) is also called a discrete Stokes complex. The vector element $\mathbb{V}_k^{\text{div}}(\mathcal{T}_h; \mathbf{r}_1)$ is H^1 -conforming and can be used as the velocity space in discretization of Stokes equation.

Lemma 4.1. *Let $r_1^e \geq 0$, $r_1^v \geq 2r_1^e + 1$, $k \geq 2r_1^v + 2$, and let $\mathbf{r}_0 = \mathbf{r}_1 + 1$, $\mathbf{r}_2 = \mathbf{r}_1 - 1$. Write*

$$\begin{aligned} \dim \mathbb{V}_{k+1}^{\text{curl}}(\mathcal{T}_h; \mathbf{r}_0) &= C_{00}|\Delta_0(\mathcal{T}_h)| + C_{01}|\Delta_1(\mathcal{T}_h)| + C_{02}|\Delta_2(\mathcal{T}_h)|, \\ \dim \mathbb{V}_k^{\text{div}}(\mathcal{T}_h; \mathbf{r}_1) &= C_{10}|\Delta_0(\mathcal{T}_h)| + C_{11}|\Delta_1(\mathcal{T}_h)| + C_{12}|\Delta_2(\mathcal{T}_h)|, \\ \dim \mathbb{V}_{k-1}^{L^2}(\mathcal{T}_h; \mathbf{r}_2) &= C_{20}|\Delta_0(\mathcal{T}_h)| + C_{21}|\Delta_1(\mathcal{T}_h)| + C_{22}|\Delta_2(\mathcal{T}_h)|. \end{aligned}$$

The coefficients C_{ij} are presented in the following table

	$ \Delta_0(\mathcal{T}_h) $	$ \Delta_1(\mathcal{T}_h) $	$ \Delta_2(\mathcal{T}_h) $
$\dim \mathbb{V}_{k+1}^{\text{curl}}(\mathcal{T}_h; \mathbf{r}_0)$	$\binom{r_0^v+2}{2}$	$\sum_{i=0}^{r_0^e} (k - 2r_0^v + i)$	$\binom{k+3}{2} - 3(C_{00} + C_{01})$
$\dim \mathbb{V}_k^{\text{div}}(\mathcal{T}_h; \mathbf{r}_1)$	$2\binom{r_1^v+2}{2}$	$2\sum_{i=0}^{r_1^e} (k - 1 - 2r_1^v + i)$	$2\binom{k+2}{2} - 3(C_{10} + C_{11})$
$\dim \mathbb{V}_{k-1}^{L^2}(\mathcal{T}_h; \mathbf{r}_2)$	$\binom{r_2^v+2}{2}$	$\sum_{i=0}^{r_2^e} (k - 2 - 2r_2^v + i)$	$\binom{k+1}{2} - 3(C_{20} + C_{21})$
$C_{0i} - C_{1i} + C_{2i}$	1	-1	1

Proof. The dimension related to $|\Delta_0(\mathcal{T}_h)|$ and $C_{00} - C_{10} + C_{20} = 1$, can be verified directly. For the column of $|\Delta_1(\mathcal{T}_h)|$, by removing the same $k - 1 - 2r_1^v$, we compute

$$C_{01} - C_{11} + C_{21} = \sum_{i=0}^{r_0^e} (i - 1) - 2 \sum_{i=0}^{r_1^e} i + \sum_{i=0}^{r_2^e} (i + 1) = -1.$$

With these two identities, the third column is an easy consequence of (13). \square

As a corollary, we obtain the following polynomial bubble complex.

Corollary 4.2. *Let $r_1^e \geq 0$, $r_1^v \geq 2r_1^e + 1$, $k \geq 2r_1^v + 2$, and let $\mathbf{r}_0 = \mathbf{r}_1 + 1$, $\mathbf{r}_2 = \mathbf{r}_1 - 1$. The polynomial bubble complex*

$$(26) \quad 0 \xrightarrow{\subset} \mathbb{B}_{k+1}(\mathbf{r}_0) \xrightarrow{\text{curl}} \mathbb{B}_k^2(\mathbf{r}_1) \xrightarrow{\text{div}} \mathbb{B}_{k-1}(\mathbf{r}_2) \xrightarrow{Q_0} \mathbb{R} \rightarrow 0$$

is exact, where Q_0 is the L^2 -projection onto the constant space.

Proof. Clearly we have $\text{curl} \mathbb{B}_{k+1}(\mathbf{r}_0) \subseteq \mathbb{B}_k^2(\mathbf{r}_1) \cap \ker(\text{div})$. For $\mathbf{v} \in \mathbb{B}_k^2(\mathbf{r}_1) \cap \ker(\text{div})$, apply complex (12) to get $\mathbf{v} = \text{curl} q$ with $q \in \mathbb{P}_{k+1}(T)$. As $\text{curl} q \in \mathbb{B}_k^2(\mathbf{r}_1)$, we have $(\text{curl} q)|_{\partial T} = 0$, which means $q|_{\partial T}$ is constant. Hence by subtracting a constant, we

can choose $q \in \mathbb{P}_{k+1}(T)$ to satisfy $q|_{\partial T} = 0$, as a result $q \in \mathbb{B}_{k+1}(\mathbf{r}_0)$. This proves $\text{curl} \mathbb{B}_{k+1}(\mathbf{r}_0) = \mathbb{B}_k^2(\mathbf{r}_1) \cap \ker(\text{div})$.

Thanks to the last column of the table in Lemma 4.1,

$$\dim \mathbb{B}_{k+1}(\mathbf{r}_0) - \dim \mathbb{B}_k^2(\mathbf{r}_1) + \dim \mathbb{B}_{k-1}(\mathbf{r}_2) - 1 = 0,$$

which together with Lemma 2.1 concludes the exactness of bubble complex (26). \square

Theorem 4.3. *Let $r_1^e \geq 0, r_1^v \geq 2r_1^e + 1, k \geq 2r_1^v + 2$, and let $\mathbf{r}_0 = \mathbf{r}_1 + 1, \mathbf{r}_2 = \mathbf{r}_1 - 1$. The finite element complex*

$$(27) \quad \mathbb{R} \xrightarrow{\subset} \mathbb{V}_{k+1}^{\text{curl}}(\mathcal{T}_h; \mathbf{r}_0) \xrightarrow{\text{curl}} \mathbb{V}_k^{\text{div}}(\mathcal{T}_h; \mathbf{r}_1) \xrightarrow{\text{div}} \mathbb{V}_{k-1}^{L^2}(\mathcal{T}_h; \mathbf{r}_2) \rightarrow 0$$

is exact.

Proof. By construction (27) is a complex, and

$$\text{curl} \mathbb{V}_{k+1}^{\text{curl}}(\mathcal{T}_h; \mathbf{r}_0) = \mathbb{V}_k^{\text{div}}(\mathcal{T}_h; \mathbf{r}_1) \cap \ker(\text{div}).$$

By Lemma 4.1 and the Euler's formula,

$$\begin{aligned} 1 - \dim \mathbb{V}_{k+1}^{\text{curl}}(\mathcal{T}_h; \mathbf{r}_0) + \dim \mathbb{V}_k^{\text{div}}(\mathcal{T}_h; \mathbf{r}_1) - \dim \mathbb{V}_{k-1}^{L^2}(\mathcal{T}_h; \mathbf{r}_2) \\ = 1 - |\Delta_0(\mathcal{T}_h)| + |\Delta_1(\mathcal{T}_h)| - |\Delta_2(\mathcal{T}_h)| = 0. \end{aligned}$$

Therefore the exactness of complex (27) follows from Lemma 2.1. \square

Example 4.4. The two-dimensional finite element de Rham complexes constructed by Falk and Neilan [22] correspond to the case $r_1^e = 0, r_1^v = 1$, and $k \geq 4$:

$$\mathbb{R} \xrightarrow{\subset} \text{Argy}_{k+1}\left(\begin{pmatrix} 2 \\ 1 \end{pmatrix}\right) \xrightarrow{\text{curl}} \text{Herm}_k\left(\begin{pmatrix} 1 \\ 0 \end{pmatrix}\right) \xrightarrow{\text{div}} \mathbb{V}_{k-1}^{L^2}\left(\begin{pmatrix} 0 \\ -1 \end{pmatrix}\right) \rightarrow 0.$$

To fit the space, we skip \mathcal{T}_h in the notation and write $\mathbf{r}_i = \begin{pmatrix} r_i^v \\ r_i^e \end{pmatrix}$ as column vectors.

The vector element is C^0 and thus the previous finite element is C^1 for which the lowest degree is the Argyris element with shape function space \mathbb{P}_5 . The last one is discontinuous \mathbb{P}_3 but continuous at vertices. If we want to use a continuous element for the pressure, i.e., $\mathbf{r}_2 = (2, 0)$, then $\mathbf{r}_1 = (3, 1), \mathbf{r}_0 = (4, 2)$ and $k \geq 8$, which may find an application in the strain gradient elasticity problem [17, 32]. Later on, we will relax the relation $\mathbf{r}_2 = \mathbf{r}_1 - 1$ and construct relative low degree Stokes pair with continuous pressure elements.

Notice that the pair $\mathbf{r}_1 = (0, 0)$ and $\mathbf{r}_2 = (-1, -1)$ are not allowed since $\mathbf{r}_0 = \mathbf{r}_1 + 1 = (1, 1)$ cannot define a C^1 element. Indeed the div stability for Stokes pair Lagrange $_k$ - DG $_{k-1}$ is more subtle and not covered in our framework.

4.2. Normal continuous finite elements for vector functions. We continue to consider the case $r_1^e = -1$ and the smoothness on edges are fixed by:

$$r_0^e = 0, \quad r_1^e = -1, \quad r_2^e = -1.$$

The constraints on the vertex smoothness are

$$r_0^v = r_1^v + 1, \quad r_1^v \geq -1, \quad r_2^v = \max\{r_1^v - 1, -1\}.$$

The finite element spaces for scalar functions $\mathbb{V}_{k+1}^{\text{curl}}(\mathcal{T}_h; \mathbf{r}_0)$ and $\mathbb{V}_{k-1}^{L^2}(\mathcal{T}_h; \mathbf{r}_2)$ remain unchanged. We need to define the finite element space for $\mathbf{H}(\text{div}, \Omega)$ with parameters $\mathbf{r}_1 = (r_1^v, -1)$. The vector function is not continuous on edges. But to be $H(\text{div})$ -conforming, the normal component should be continuous. A refined notation for the

smoothness parameter would be $\mathbf{r}_1 = \begin{pmatrix} r_1^v \\ -1, 0 \end{pmatrix}$ where the tangential component is -1 (discontinuous) and the normal component is 0 (continuous); notation $\begin{pmatrix} r_1^v \\ \frac{1}{2} \end{pmatrix}$ is adopted in [28]. To simplify notation, we still use the simplified form $\mathbf{r}_1 = (r_1^v, -1)$ and understand that $r_1^e = -1$ for $\mathbb{V}_k^{\text{div}}(\mathcal{T}_h; \mathbf{r}_1)$ space means the normal continuity.

Take $\mathbb{P}_k(T; \mathbb{R}^2)$ with $k \geq \max\{2r_1^v + 2, 1\}$ as the space of shape functions. For $r_1^v \geq 0$, the DoFs are

$$(28a) \quad \nabla^i \mathbf{v}(\mathbf{v}), \quad \mathbf{v} \in \Delta_0(T), i = 0, \dots, r_1^v,$$

$$(28b) \quad \int_e \mathbf{v} \cdot \mathbf{n} q \, ds, \quad \mathbf{q} \in \mathbb{P}_{k-2(r_1^v+1)}(e), e \in \Delta_1(T),$$

$$(28c) \quad \int_e \mathbf{v} \cdot \mathbf{t} q \, ds, \quad \mathbf{q} \in \mathbb{P}_{k-2(r_1^v+1)}(e), e \in \Delta_1(T),$$

$$(28d) \quad \int_T \mathbf{v} \cdot \mathbf{q} \, dx, \quad \mathbf{q} \in \mathbb{B}_k^2((r_1^v, 0)).$$

Although $r_1^e = -1$, we still use $\mathbb{B}_k((r_1^v, 0))$ not $\mathbb{B}_k((r_1^v, -1))$ as the interior moments so that we can have DoFs (28b)-(28c) on edges. Namely locally we use the vector Hermite-type element with parameter $(r_1^v, 0)$. When defining the global $H(\text{div})$ -conforming finite element space, the tangential component (28c) is considered as local, i.e., double valued on interior edges.

When $r_1^v = -1$, there is no DoFs on vertices and DoFs are

$$(29a) \quad \int_e \mathbf{v} \cdot \mathbf{n} q \, ds, \quad \mathbf{q} \in \mathbb{P}_k(e), e \in \Delta_1(T),$$

$$(29b) \quad \int_e \mathbf{v} \cdot \mathbf{t} q \, ds, \quad \mathbf{q} \in \mathbb{P}_{k-2}(e), e \in \Delta_1(T),$$

$$(29c) \quad \int_T \mathbf{v} \cdot \mathbf{q} \, dx, \quad \mathbf{q} \in \mathbb{B}_k^2((0, 0)).$$

The normal component is the full degree polynomial $\mathbb{P}_k(e)$ but the tangential component is corresponding to the edge bubble $b_e \mathbb{P}_{k-2}(e)$. The interior moments become $\mathbb{B}_k((0, 0))$. Locally we use vector Lagrange finite element. At each edge, we use $t - n$ (tangential-normal) coordinate and at a vertex we use the coordinate formed by the two normal direction of two edges containing that vertex and merge into (29a). Then the uni-solvence in one triangle follows from that of vector Lagrange elements.

Define the global $H(\text{div})$ -conforming finite element space

$$\mathbb{V}_k^{\text{div}}(\mathcal{T}_h; (r_1^v, -1)) = \{\mathbf{v} \in \mathbf{L}^2(\Omega; \mathbb{R}^2) : \mathbf{v}|_T \in \mathbb{P}_k(T; \mathbb{R}^2) \forall T \in \mathcal{T}_h, \\ \text{all the DoFs (28a)-(28b) are single-valued}\},$$

for $r_1^v \geq 0$, and

$$\mathbb{V}_k^{\text{div}}(\mathcal{T}_h; (-1, -1)) = \{\mathbf{v} \in \mathbf{L}^2(\Omega; \mathbb{R}^2) : \mathbf{v}|_T \in \mathbb{P}_k(T; \mathbb{R}^2) \forall T \in \mathcal{T}_h, \\ \text{DoF (29a) is single-valued}\},$$

where the tangential component (28c) and (29b) are considered as local and may be double-valued for each interior edge.

Theorem 4.5. *Assume parameters $\mathbf{r}_0, \mathbf{r}_1, \mathbf{r}_2$ satisfy*

$$\begin{aligned} r_0^v &= r_1^v + 1, & r_1^v &\geq -1, & r_2^v &= \max\{r_1^v, 0\} - 1, \\ r_0^e &= 0, & r_1^e &= -1, & r_2^e &= -1. \end{aligned}$$

Let $k \geq \max\{2r_1^v + 2, 1\}$. The finite element complex

$$(30) \quad \mathbb{R} \xrightarrow{\subset} \mathbb{V}_{k+1}^{\text{curl}}(\mathcal{T}_h; \mathbf{r}_0) \xrightarrow{\text{curl}} \mathbb{V}_k^{\text{div}}(\mathcal{T}_h; \mathbf{r}_1) \xrightarrow{\text{div}} \mathbb{V}_{k-1}^{L^2}(\mathcal{T}_h; \mathbf{r}_2) \rightarrow 0$$

is exact.

Proof. Apparently (30) is a complex, and

$$\text{curl } \mathbb{V}_{k+1}^{\text{curl}}(\mathcal{T}_h; \mathbf{r}_0) = \mathbb{V}_k^{\text{div}}(\mathcal{T}_h; \mathbf{r}_1) \cap \ker(\text{div}).$$

Then we count the dimension. The dimension count in Lemma 4.1 is still valid except $C_{11} = k - 1 - 2r_1^v$. As $C_{01} = k - 2r_0^v$ and $C_{21} = 0$, the identity $C_{01} - C_{11} + C_{21} = -1$ still holds. The rest of the proof is the same as that of Theorem 4.3. \square

Example 4.6. For $k \geq 1$, $r_0^v = 0, r_1^v = -1, r_2^v = -1$, we recover the standard finite element de Rham complex

$$\mathbb{R} \xrightarrow{\subset} \text{Lagrange}_{k+1}\left(\begin{pmatrix} 0 \\ 0 \end{pmatrix}\right) \xrightarrow{\text{curl}} \text{BDM}_k\left(\begin{pmatrix} -1 \\ -1 \end{pmatrix}\right) \xrightarrow{\text{div}} \text{DG}_{k-1}\left(\begin{pmatrix} -1 \\ -1 \end{pmatrix}\right) \rightarrow 0.$$

We can choose $r_0^v = 1, r_1^v = 0, r_2^v = -1$ and $k \geq 2$ to get

$$\mathbb{R} \xrightarrow{\subset} \text{Herm}_{k+1}\left(\begin{pmatrix} 1 \\ 0 \end{pmatrix}\right) \xrightarrow{\text{curl}} \text{Sten}_k\left(\begin{pmatrix} 0 \\ -1 \end{pmatrix}\right) \xrightarrow{\text{div}} \text{DG}_{k-1}\left(\begin{pmatrix} -1 \\ -1 \end{pmatrix}\right) \rightarrow 0,$$

which has been constructed in [19].

4.3. General cases with inequality constraint. We consider more general cases with an inequality constraint on the smoothness parameters \mathbf{r}_1 and \mathbf{r}_2 :

$$(31) \quad \mathbf{r}_0 = \mathbf{r}_1 + 1, \quad \mathbf{r}_1 \geq -1, \quad \mathbf{r}_2 \geq \mathbf{r}_1 \ominus 1, \quad r_1^v \geq 2r_1^e + 1, \quad r_2^v \geq 2r_2^e.$$

To define the finite element spaces, we further require

$$k \geq \max\{2r_1^v + 2, 2r_2^v + 2, 3r_2^e + 4, (r_2^e + 4)[r_2^v = 0]\},$$

where the Iverson bracket $[\text{statement}] = 1$ if the statement inside the bracket is true and 0 otherwise.

The finite element spaces for scalar functions $\mathbb{V}_{k+1}^{\text{curl}}(\mathcal{T}_h; \mathbf{r}_0)$ and $\mathbb{V}_{k-1}^{L^2}(\mathcal{T}_h; \mathbf{r}_2)$ remain unchanged. Next we define a new finite element space for $\mathbf{H}(\text{div}, \Omega)$. Take $\mathbb{P}_k(T; \mathbb{R}^2)$ as

the space of shape functions. The degrees of freedom are

$$(32a) \quad \nabla^i \mathbf{v}(\mathbf{v}), \quad \mathbf{v} \in \Delta_0(T), i = 0, \dots, r_1^v,$$

$$(32b) \quad \nabla^j \operatorname{div} \mathbf{v}(\mathbf{v}), \quad \mathbf{v} \in \Delta_0(T), j = \max\{r_1^v, 0\}, \dots, r_2^v,$$

$$(32c) \quad \int_e \mathbf{v} \cdot \mathbf{n} q \, ds, \quad q \in \mathbb{P}_{k-2(r_1^v+1)}(e), e \in \Delta_1(T),$$

$$(32d) \quad \int_e \partial_n^i(\mathbf{v} \cdot \mathbf{t}) q \, ds, \quad q \in \mathbb{P}_{k-2(r_1^v+1)+i}(e), e \in \Delta_1(T), i = 0, \dots, r_1^e,$$

$$(32e) \quad \int_e \partial_n^i(\operatorname{div} \mathbf{v}) q \, ds, \quad q \in \mathbb{P}_{k-1-2(r_2^v+1)+i}(e), e \in \Delta_1(T), i = 0, \dots, r_2^e,$$

$$(32f) \quad \int_T \operatorname{div} \mathbf{v} q \, dx, \quad q \in \mathbb{B}_{k-1}(\mathbf{r}_2)/\mathbb{R},$$

$$(32g) \quad \int_T \mathbf{v} \cdot \mathbf{q} \, dx, \quad \mathbf{q} \in \operatorname{curl} \mathbb{B}_{k+1}(\mathbf{r}_1 + 1).$$

We explain the change of DoFs. We add DoFs (32b), (32e), and (32f) on $\operatorname{div} \mathbf{v}$ to determine $\operatorname{div} \mathbf{v} \in \mathbb{V}_{k-1}^{L^2}(\mathcal{T}_h; \mathbf{r}_2)$. For interior moments, we use the bubble complex (26) to split it into range of div and its orthogonal complement. On edges, DoFs on $\operatorname{div} \mathbf{v}$ introduce some linear dependence of normal derivatives of the tangential and normal components and thus need to remove some redundancy.

More precisely, for $i = 0, 1, \dots, r_1^e - 1$ with $r_2^e = r_1^e - 1 \geq 0$,

$$\partial_n^i(\operatorname{div} \mathbf{v}) = \partial_n^i(\partial_n(\mathbf{v} \cdot \mathbf{n}) + \partial_t(\mathbf{v} \cdot \mathbf{t})) = \partial_n^{i+1}(\mathbf{v} \cdot \mathbf{n}) + \partial_t(\partial_n^i(\mathbf{v} \cdot \mathbf{t})).$$

The second term $\partial_t(\partial_n^i(\mathbf{v} \cdot \mathbf{t}))$ will be determined by (32a) and (32d). The normal derivative of the normal component $\partial_n^{i+1}(\mathbf{v} \cdot \mathbf{n})$, $i \geq 0$, is built into (32e) but not $\mathbf{v} \cdot \mathbf{n}$ which should be explicitly included in (32c). A linear combination of (32c), (32d), and (32e) will determine

$$\int_e \partial_n^i \mathbf{v} \cdot \mathbf{q} \, ds, \quad \mathbf{q} \in \mathbb{P}_{k-2(r_1^v+1)+i}^2(e), e \in \Delta_1(T_h), i = 0, 1, \dots, r_1^e.$$

Consequently it returns to the smooth finite elements defined before.

Lemma 4.7. *Assume $\mathbf{r}_1, \mathbf{r}_2$ satisfy (31), and $k \geq \max\{2r_2^v + 2, 3r_2^e + 4, (r_2^e + 4)[r_2^v = 0]\}$. The DoFs (32a)-(32g) are uni-solvent for $\mathbb{P}_k(T; \mathbb{R}^2)$.*

Proof. The condition $k \geq \max\{2r_2^v + 2, 3r_2^e + 4, (r_2^e + 4)[r_2^v = 0]\}$ ensures $\dim \mathbb{B}_{k-1}(\mathbf{r}_2) \geq 1$ which can be verified by showing $|S_2(T)| > 0$ cf. Lemma 3.5.

The number of DoFs (32b) and (32e)-(32f) on $\operatorname{div} \mathbf{v}$ is $\dim \mathbb{P}_{k-1}(T) - 3\binom{r_1^v+1}{2} - 1$, which is constant with respect to \mathbf{r}_2 . Hence the number of DoFs (32a)-(32g) is also constant with respect to \mathbf{r}_2 . As a result the number of DoFs (32a)-(32g) equals to $\dim \mathbb{P}_k(T; \mathbb{R}^2)$, which has been proved for case $\mathbf{r}_2 = \mathbf{r}_1 \ominus 1$.

Take $\mathbf{v} \in \mathbb{P}_k(T; \mathbb{R}^2)$ and assume all the DoFs (32a)-(32g) vanish. The vanishing DoF (32c) implies $\operatorname{div} \mathbf{v} \in L_0^2(T)$. By the vanishing DoFs (32a)-(32b) and (32e)-(32f), we get $\operatorname{div} \mathbf{v} = 0$. And it follows from the vanishing DoFs (32a) and (32c)-(32d) that $\mathbf{v} \in \operatorname{curl} \mathbb{B}_{k+1}(\mathbf{r}_1 + 1)$. Therefore $\mathbf{v} = \mathbf{0}$ holds from the vanishing DoF (32g). \square

Define global $C^{r_1^e}$ -continuous finite element space

$$\mathbb{V}_k^{\operatorname{div}}(\mathcal{T}_h; \mathbf{r}_1, \mathbf{r}_2) = \{\mathbf{v} \in \mathbf{L}^2(\Omega; \mathbb{R}^2) : \mathbf{v}|_T \in \mathbb{P}_k(T; \mathbb{R}^2) \forall T \in \mathcal{T}_h,$$

all the DoFs (32a)-(32e) are single-valued\}.

When $\mathbf{r}_2 \geq \mathbf{r}_1 \ominus 1$, we have

$$\mathbb{V}_k^{\text{div}}(\mathcal{T}_h; \mathbf{r}_1, \mathbf{r}_2) \subseteq \mathbb{V}_k^{\text{div}}(\mathcal{T}_h; \mathbf{r}_1, \mathbf{r}_1 \ominus 1).$$

Namely additional smoothness on $\text{div } \mathbf{v}$ is imposed. We use Figure 3 to illustrate the exactness of the finite element de Rham complex (33), which is obtained by adding more constraints on $\text{div } \mathbf{v}$.

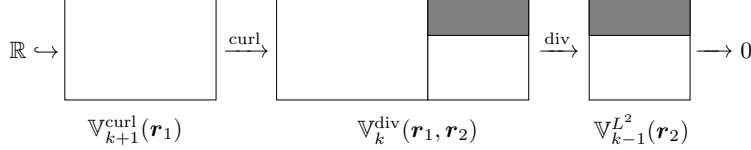


FIGURE 3. Explanation of the smooth finite element de Rham complex with increased smoothness in pressure.

Theorem 4.8. *Let $\mathbf{r}_0 = \mathbf{r}_1 + 1$, $\mathbf{r}_1 \geq -1$, $\mathbf{r}_2 \geq \mathbf{r}_1 \ominus 1$ satisfying $r_1^v \geq 2r_1^e + 1$, $r_2^v \geq 2r_2^e$. Assume $k \geq \max\{2r_1^v + 2, 2r_2^v + 2, 3r_2^e + 4, (r_2^e + 4)[r_2^v = 0]\}$. The finite element complex*

$$(33) \quad \mathbb{R} \xrightarrow{\subset} \mathbb{V}_{k+1}^{\text{curl}}(\mathcal{T}_h; \mathbf{r}_0) \xrightarrow{\text{curl}} \mathbb{V}_k^{\text{div}}(\mathcal{T}_h; \mathbf{r}_1, \mathbf{r}_2) \xrightarrow{\text{div}} \mathbb{V}_{k-1}^{L^2}(\mathcal{T}_h; \mathbf{r}_2) \rightarrow 0$$

is exact.

Proof. It is straightforward to verify that (33) is a complex by showing $\text{curl } \mathbb{V}_{k+1}^{\text{curl}}(\mathcal{T}_h; \mathbf{r}_0) \subseteq \mathbb{V}_k^{\text{div}}(\mathcal{T}_h; \mathbf{r}_1, \mathbf{r}_2)$ and $\text{div } \mathbb{V}_k^{\text{div}}(\mathcal{T}_h; \mathbf{r}_1, \mathbf{r}_2) \subseteq \mathbb{V}_{k-1}^{L^2}(\mathcal{T}_h; \mathbf{r}_2)$. It is also obvious that

$$\text{curl } \mathbb{V}_{k+1}^{\text{curl}}(\mathcal{T}_h; \mathbf{r}_0) = \mathbb{V}_k^{\text{div}}(\mathcal{T}_h; \mathbf{r}_1, \mathbf{r}_2) \cap \ker(\text{div}).$$

We have proved the exactness for $\mathbf{r}_2 = \mathbf{r}_1 \ominus 1$. When counting the dimension, only need to check the difference.

The added vertex DoFs for $\mathbb{V}_k^{\text{div}}(\mathcal{T}_h; \mathbf{r}_1, \mathbf{r}_2)$ and $\mathbb{V}_{k-1}^{L^2}(\mathcal{T}_h; \mathbf{r}_2)$ are equal, i.e.,

$$C_{10}(\mathbf{r}_2) - C_{10}(\mathbf{r}_1 \ominus 1) = C_{20}(\mathbf{r}_2) - C_{20}(\mathbf{r}_1 \ominus 1).$$

Same argument can be applied to edge DoFs. Therefore the alternating column sums remain the same and the proof of Theorem 4.3 can be still applied. \square

We present two examples of the de Rham complex ending with the Lagrange element.

Example 4.9. Consider the case $\mathbf{r}_1 = (1, 0)$, $\mathbf{r}_2 = 0$ and $k \geq 4$, which is also constructed as $H^1(\text{div}) - H^1$ Stokes pair in Falk and Neilan [22]. Now we can choose continuous pressure space without increasing the polynomial degree. The complex is

$$\mathbb{R} \xrightarrow{\subset} \text{Argv}_{k+1} \left(\begin{pmatrix} 2 \\ 1 \end{pmatrix} \right) \xrightarrow{\text{curl}} \mathbb{V}_k^{\text{div}} \left(\begin{pmatrix} 1 \\ 0 \end{pmatrix}, \begin{pmatrix} 0 \\ 0 \end{pmatrix} \right) \xrightarrow{\text{div}} \text{Lagrange}_{k-1} \left(\begin{pmatrix} 0 \\ 0 \end{pmatrix} \right) \rightarrow 0.$$

The velocity space is a reduced Hermite space with continuity of $\text{div } \mathbf{v}$ at vertices and edges. With such modification, this $\mathbb{P}_k - \mathbb{P}_{k-1}$ Stokes pair with continuous pressure element is point-wise divergence free comparing to the Taylor-Hood element.

Example 4.10. Consider the case $\mathbf{r}_1 = -1$ and $\mathbf{r}_2 = 0$, and $k \geq 4$. The complex is

$$\mathbb{R} \xrightarrow{\subset} \text{Lagrange}_{k+1} \left(\begin{pmatrix} 0 \\ 0 \end{pmatrix} \right) \xrightarrow{\text{curl}} \mathbb{V}_k^{\text{div}} \left(\begin{pmatrix} -1 \\ -1 \end{pmatrix}, \begin{pmatrix} 0 \\ 0 \end{pmatrix} \right) \xrightarrow{\text{div}} \text{Lagrange}_{k-1} \left(\begin{pmatrix} 0 \\ 0 \end{pmatrix} \right) \rightarrow 0,$$

which is the rotation of the finite element de Rham complex in [30, Section 5.2.1]. The space $\mathbb{V}_k^{\text{div}}(\mathcal{T}_h; \mathbf{r}_1, \mathbf{r}_0)$ can be used to discretize fourth-order div or curl equations [23, 30]. We can also apply the pair $\mathbb{V}_k^{\text{div}}(\mathcal{T}_h; \mathbf{r}_1, \mathbf{r}_0)$ and $\text{Lagrange}_{k-1}(\mathcal{T}_h; \mathbf{r}_0)$ to mixed finite element methods for Poisson equation $-\Delta u = f$, in which the discrete u_h is continuous.

For simplicity, hereafter we will omit the triangulation \mathcal{T}_h in the notation of global finite element spaces. For example, $\mathbb{V}_k^{\text{div}}(\mathcal{T}_h; \mathbf{r}_1, \mathbf{r}_2)$ will be abbreviated as $\mathbb{V}_k^{\text{div}}(\mathbf{r}_1, \mathbf{r}_2)$.

5. BEYOND THE DE RHAM COMPLEX

In this section, we shall construct more finite element complexes from copies of finite element de Rham complexes.

5.1. Finite element curl div complexes. Based on the finite element de Rham complex (33), we can obtain the finite element discretization of the curl div complex [7]

$$\mathbb{R} \times \{0\} \xrightarrow{c} H^1(\Omega) \times \mathbb{R} \xrightarrow{(\text{curl}, \mathbf{x})} \mathbf{H}(\text{curl div}, \Omega) \xrightarrow{\text{curl div}} \mathbf{H}(\text{div}, \Omega) \xrightarrow{\text{div}} L^2(\Omega) \rightarrow 0,$$

where $\mathbf{H}(\text{curl div}, \Omega) := \mathbf{H}^{0,1}(\text{div}, \Omega) = \{\mathbf{v} \in \mathbf{H}(\text{div}, \Omega) : \text{div } \mathbf{v} \in H^1(\Omega)\}$, and the operator $(\text{curl}, \mathbf{x})$ is defined by $(\text{curl}, \mathbf{x}) \begin{pmatrix} v \\ c \end{pmatrix} := \text{curl } v + c\mathbf{x}$ for $v \in H^1(\Omega)$ and $c \in \mathbb{R}$.

Theorem 5.1. *Let $\mathbf{r}_0 = \mathbf{r}_1 + 1$, $\mathbf{r}_1 \geq -1$, $\mathbf{r}_2 \geq \max\{\mathbf{r}_1 - 1, 0\}$, $\mathbf{r}_3 \geq \max\{\mathbf{r}_2 - 2, -1\}$ satisfying $r_1^v \geq 2r_1^e + 1$, $r_2^v \geq 2r_2^e$, $r_3^v \geq 2r_3^e$. Assume $k \geq \max\{2r_1^v + 2, 2r_2^v + 2, 3r_2^e + 4, (r_2^e + 4)[r_2^v = 0], 2r_3^v + 4, 3r_3^e + 6, (r_3^e + 6)[r_3^v = 0]\}$. The finite element complex*

$$(34) \quad \mathbb{R} \times \{0\} \xrightarrow{c} \mathbb{V}_{k+1}^{\text{curl}}(\mathbf{r}_0) \times \mathbb{R} \xrightarrow{(\text{curl}, \mathbf{x})} \mathbb{V}_k^{\text{div}}(\mathbf{r}_1, \mathbf{r}_2) \xrightarrow{\text{curl div}} \mathbb{V}_{k-2}^{\text{div}}(\mathbf{r}_2 - 1, \mathbf{r}_3) \xrightarrow{\text{div}} \mathbb{V}_{k-3}^{L^2}(\mathbf{r}_3) \rightarrow 0$$

is exact.

Proof. By complex (33), clearly (34) is a complex, and $\text{div } \mathbb{V}_{k-2}^{\text{div}}(\mathbf{r}_2 - 1, \mathbf{r}_3) = \mathbb{V}_{k-3}^{L^2}(\mathbf{r}_3)$. We will focus on the exactness of complex (34).

The condition $k \geq \max\{2r_2^v + 2, 3r_2^e + 4, (r_2^e + 4)[r_2^v = 0]\}$ implies $\dim \mathbb{B}_{k-1}(\mathbf{r}_2) \geq 1$, and $k \geq \max\{2r_3^v + 4, 3r_3^e + 6, (r_3^e + 6)[r_3^v = 0]\}$ implies $\dim \mathbb{B}_{k-3}(\mathbf{r}_3) \geq 1$. We get from the exactness of complex (33) that

$$\text{div } \mathbb{V}_k^{\text{div}}(\mathbf{r}_1, \mathbf{r}_2) = \mathbb{V}_{k-1}^{L^2}(\mathbf{r}_2), \quad \text{curl } \mathbb{V}_{k-1}^{\text{curl}}(\mathbf{r}_2) = \mathbb{V}_{k-2}^{\text{div}}(\mathbf{r}_2 - 1, \mathbf{r}_3) \cap \ker(\text{div}).$$

Hence $\text{curl div } \mathbb{V}_k^{\text{div}}(\mathbf{r}_1, \mathbf{r}_2) = \mathbb{V}_{k-2}^{\text{div}}(\mathbf{r}_2 - 1, \mathbf{r}_3) \cap \ker(\text{div})$ follows from $\mathbb{V}_{k-1}^{\text{curl}}(\mathbf{r}_2) = \mathbb{V}_{k-1}^{L^2}(\mathbf{r}_2)$ when $\mathbf{r}_2 \geq 0$.

For $\mathbf{v} \in \mathbb{V}_k^{\text{div}}(\mathbf{r}_1, \mathbf{r}_2) \cap \ker(\text{curl div})$, there exists constant c such that $\text{div } \mathbf{v} = 2c$. Then we have $\text{div}(\mathbf{v} - c\mathbf{x}) = 0$, i.e., $\mathbf{v} - c\mathbf{x} \in \mathbb{V}_k^{\text{div}}(\mathbf{r}_1, \mathbf{r}_2) \cap \ker(\text{div})$. Therefore $\mathbf{v} \in \text{curl } \mathbb{V}_{k+1}^{\text{curl}}(\mathbf{r}_0) \oplus \mathbf{x}\mathbb{R}$ holds from the exactness of complex (33). \square

5.2. Finite element elasticity and Hessian complexes. We first present two examples. Denote by

$$\mathbb{V}_k^{\text{div}}(\mathbf{r}_1, \mathbf{r}_2; \mathbb{M}) := \mathbb{V}_k^{\text{div}}(\mathbf{r}_1, \mathbf{r}_2) \times \mathbb{V}_k^{\text{div}}(\mathbf{r}_1, \mathbf{r}_2).$$

We take two vector functions by row to form a matrix and each row belongs to $\mathbb{V}_k^{\text{div}}(\mathbf{r}_1, \mathbf{r}_2)$. To fit the space, we skip the constant space \mathbb{R} in the beginning and 0 at the end in the sequence, and \mathcal{T}_h in the spaces. The first example has been presented in [19] for $k \geq 3$:

$$\begin{array}{ccccc} \text{Argy}_{k+2}\left(\begin{pmatrix} 2 \\ 1 \end{pmatrix}\right) & \xrightarrow{\text{curl}} & \text{Herm}_{k+1}\left(\begin{pmatrix} 1 \\ 0 \end{pmatrix}; \mathbb{R}^2\right) & \xrightarrow{\text{div}} & \mathbb{V}_k^{L^2}\left(\begin{pmatrix} 0 \\ -1 \end{pmatrix}\right) \\ & \nearrow \text{id} & & \nearrow -2 \text{sskw} & \\ \text{Herm}_{k+1}\left(\begin{pmatrix} 1 \\ 0 \end{pmatrix}; \mathbb{R}^2\right) & \xrightarrow{\text{curl}} & \text{Sten}_k\left(\begin{pmatrix} 0 \\ -1 \end{pmatrix}; \mathbb{M}\right) & \xrightarrow{\text{div}} & \text{DG}_{k-1}\left(\begin{pmatrix} -1 \\ -1 \end{pmatrix}; \mathbb{R}^2\right) \end{array}$$

This will lead to the elasticity complex

$$(35) \quad \mathbf{RM} \xrightarrow{\subset} \text{Argy}_{k+2}\left(\begin{pmatrix} 2 \\ 1 \end{pmatrix}\right) \xrightarrow{\text{Air}} \text{HZ}_k\left(\begin{pmatrix} 0 \\ -1 \end{pmatrix}; \mathbb{S}\right) \xrightarrow{\text{div}} \text{DG}_{k-1}\left(\begin{pmatrix} -1 \\ -1 \end{pmatrix}; \mathbb{R}^2\right) \rightarrow \mathbf{0}.$$

We then present another example with rotated differential operators and use $\mathbb{V}^{\text{rot}}(\mathbf{r}_1, \mathbf{r}_2)$ to increase the smoothness of the last space. The finite element BGG diagram for $k \geq 5$

$$\begin{array}{ccccc} \text{Argy}_{k+2}\left(\begin{pmatrix} 2 \\ 1 \end{pmatrix}\right) & \xrightarrow{\text{grad}} & \text{Herm}_{k+1}\left(\begin{pmatrix} 1 \\ 0 \end{pmatrix}; \mathbb{R}^2\right) & \xrightarrow{\text{rot}} & \mathbb{V}_k^{L^2}\left(\begin{pmatrix} 0 \\ -1 \end{pmatrix}\right) \\ & \nearrow \text{id} & & \nearrow -2 \text{sskw} & \\ \text{Herm}_{k+1}\left(\begin{pmatrix} 1 \\ 0 \end{pmatrix}; \mathbb{R}^2\right) & \xrightarrow{\text{grad}} & \mathbb{V}_k^{\text{rot}}\left(\begin{pmatrix} 0 \\ -1 \end{pmatrix}, \begin{pmatrix} 0 \\ 0 \end{pmatrix}; \mathbb{M}\right) & \xrightarrow{\text{rot}} & \text{Lagrange}_{k-1}\left(\begin{pmatrix} 0 \\ 0 \end{pmatrix}; \mathbb{R}^2\right) \end{array}$$

will lead to the finite element Hessian complex constructed in [15]

$$(36) \quad \mathbb{P}_1 \xrightarrow{\subset} V_{k+2}^{\text{hess}} \xrightarrow{\nabla^2} \Sigma_k^{\text{rot}} \xrightarrow{\text{rot}} V_{k-1}^{\text{grad}} \rightarrow \mathbf{0}.$$

Note that complex (36) is not a rotation of complex (35) as complex (36) ends at a continuous Lagrange element.

We now present the general case.

Theorem 5.2. *Let $\mathbf{r}_1 \geq -1$ and $\mathbf{r}_2 \geq \mathbf{r}_1 \ominus 1$ satisfying $r_1^v \geq 2r_1^e + 2$, $r_2^v \geq 2r_2^e$, and let polynomial degree $k \geq \max\{2r_1^v + 3, 2r_2^v + 2, 3r_2^e + 5, 5[r_2^e = -1, r_2^v = 1], 3[r_2^e = -1, r_2^v = 0]\}$. Then we have the BGG diagram*

$$(37) \quad \begin{array}{ccccccc} \mathbb{R} & \xrightarrow{\subset} & \mathbb{V}_{k+2}^{\text{curl}}(\mathbf{r}_1 + 2) & \xrightarrow{\text{curl}} & \mathbb{V}_{k+1}^{\text{div}}(\mathbf{r}_1 + 1) & \xrightarrow{\text{div}} & \mathbb{V}_k^{L^2}(\mathbf{r}_1) \longrightarrow \mathbf{0} \\ & \nearrow \cdot(-\mathbf{x})^\perp & & \nearrow \text{id} & & \nearrow -2 \text{sskw} & \\ \mathbb{R}^2 & \xrightarrow{\subset} & \mathbb{V}_{k+1}^{\text{curl}}(\mathbf{r}_1 + 1; \mathbb{R}^2) & \xrightarrow{\text{curl}} & \mathbb{V}_k^{\text{div}}(\mathbf{r}_1, \mathbf{r}_2; \mathbb{M}) & \xrightarrow{\text{div}} & \mathbb{V}_{k-1}^{L^2}(\mathbf{r}_2; \mathbb{R}^2) \longrightarrow \mathbf{0} \end{array}$$

which leads to the finite element elasticity complex

$$(38) \quad \mathbb{P}_1 \xrightarrow{\subset} \mathbb{V}_{k+2}^{\text{curl}}(\mathbf{r}_1 + 2) \xrightarrow{\text{Air}} \mathbb{V}_k^{\text{div}}(\mathbf{r}_1, \mathbf{r}_2; \mathbb{S}) \xrightarrow{\text{div}} \mathbb{V}_{k-1}^{L^2}(\mathbf{r}_2; \mathbb{R}^2) \rightarrow \mathbf{0},$$

where $\mathbb{V}_k^{\text{div}}(\mathbf{r}_1, \mathbf{r}_2; \mathbb{S}) := \mathbb{V}_k^{\text{div}}(\mathbf{r}_1, \mathbf{r}_2; \mathbb{M}) \cap \ker(\text{sskw})$.

Proof. First we show that $\text{sskw } \mathbb{V}_k^{\text{div}}(\mathbf{r}_1, \mathbf{r}_2; \mathbb{M}) = \mathbb{V}_k^{L^2}(\mathbf{r}_1)$. For $q \in \mathbb{V}_k^{L^2}(\mathbf{r}_1)$, by the exactness of the complex in the top line of (37), there exists $\mathbf{v}_h \in \mathbb{V}_{k+1}^{\text{div}}(\mathbf{r}_1) = \mathbb{V}_{k+1}^{\text{curl}}(\mathbf{r}_1)$ such that $\text{div } \mathbf{v}_h = q_h$. Then we get from the anti-commutative property (7) that $q_h = 2 \text{sskw}(\text{curl } \mathbf{v}_h)$.

Again condition $k \geq \max\{2r_2^v + 2, 3r_2^e + 5, 5[r_2^e = -1, r_2^v = 1], 3[r_2^e = -1, r_2^v = 0]\}$ ensures $\dim \mathbb{B}_{k-1}(\mathbf{r}_2) \geq 3$.

We can apply the BGG framework in [7] to get the complex (38) and its exactness. In two dimensions, we will provide a simple proof without invoking the machinery.

Clearly (38) is a complex. We prove the exactness of complex (38) in two steps.

Step 1. Prove $\text{Air } \mathbb{V}_{k+2}^{\text{curl}}(\mathbf{r}_1+2) = \mathbb{V}_k^{\text{div}}(\mathbf{r}_1, \mathbf{r}_2; \mathbb{S}) \cap \ker(\text{div})$. For $\boldsymbol{\tau} \in \mathbb{V}_k^{\text{div}}(\mathbf{r}_1, \mathbf{r}_2; \mathbb{S}) \cap \ker(\text{div})$, by the bottom complex in (37), there exists $\mathbf{v} \in \mathbb{V}_{k+1}^{\text{curl}}(\mathbf{r}_1 + 1; \mathbb{R}^2)$ such that $\boldsymbol{\tau} = \text{curl } \mathbf{v}$. Then it follows from (7) that

$$\text{div } \mathbf{v} = 2 \text{sskw}(\text{curl } \mathbf{v}) = 2 \text{sskw } \boldsymbol{\tau} = 0.$$

By the exactness of the top de Rham complex, there exists $q \in \mathbb{V}_{k+2}^{\text{curl}}(\mathbf{r}_1 + 2)$ such that $\mathbf{v} = \text{curl } q$. Thus $\boldsymbol{\tau} = \text{curl } \mathbf{v} = \text{Air } q \in \text{Air } \mathbb{V}_{k+2}^{\text{curl}}(\mathbf{r}_1 + 2)$.

Step 2. Prove $\text{div } \mathbb{V}_k^{\text{div}}(\mathbf{r}_1, \mathbf{r}_2; \mathbb{S}) = \mathbb{V}_{k-1}^{L^2}(\mathbf{r}_2; \mathbb{R}^2)$. As $\text{div} : \mathbb{V}_k^{\text{div}}(\mathbf{r}_1, \mathbf{r}_2; \mathbb{M}) \rightarrow \mathbb{V}_{k-1}^{L^2}(\mathbf{r}_2; \mathbb{R}^2)$ is surjective, given a $\mathbf{q} \in \mathbb{V}_{k-1}^{L^2}(\mathbf{r}_2; \mathbb{R}^2)$, we can find $\boldsymbol{\tau} \in \mathbb{V}_k^{\text{div}}(\mathbf{r}_1, \mathbf{r}_2; \mathbb{M})$ such that $\text{div } \boldsymbol{\tau} = \mathbf{q}$. By the diagram (37), we can find $\mathbf{v} \in \mathbb{V}_{k+1}^{\text{div}}(\mathbf{r}_1 + 1)$ such that $\text{div } \mathbf{v} = -2 \text{sskw } \boldsymbol{\tau}$. Set $\boldsymbol{\tau}^s = \boldsymbol{\tau} + \text{curl } \mathbf{v}$. Then $\text{div } \boldsymbol{\tau}^s = \text{div } \boldsymbol{\tau} = \mathbf{q}$ and $2 \text{sskw } \boldsymbol{\tau}^s = 2 \text{sskw } \boldsymbol{\tau} + 2 \text{sskw } \text{curl } \mathbf{v} = 2 \text{sskw } \boldsymbol{\tau} + \text{div } \mathbf{v} = 0$, i.e. $\boldsymbol{\tau}^s$ is symmetric. Therefore we find $\boldsymbol{\tau}^s \in \mathbb{V}_k^{\text{div}}(\mathbf{r}_1, \mathbf{r}_2; \mathbb{S})$ and $\text{div } \boldsymbol{\tau}^s = \mathbf{q}$. \square

In (38), $\mathbb{V}_k^{\text{div}}(\mathbf{r}_1, \mathbf{r}_2; \mathbb{S})$ is defined as $\mathbb{V}_k^{\text{div}}(\mathbf{r}_1, \mathbf{r}_2; \mathbb{M}) \cap \ker(\text{sskw})$. Next we give the finite element description of space $\mathbb{V}_k^{\text{div}}(\mathbf{r}_1, \mathbf{r}_2; \mathbb{S})$ and thus can obtain locally supported basis. On each triangle, we take $\mathbb{P}_k(T; \mathbb{S})$ as the shape function space. By symmetrizing DoFs (32a)-(32g), we propose the following local DoFs for space $\mathbb{V}_k^{\text{div}}(\mathbf{r}_1, \mathbf{r}_2; \mathbb{S})$

$$(39a) \quad \nabla^i \boldsymbol{\tau}(\mathbf{v}), \quad \mathbf{v} \in \Delta_0(T), i = 0, \dots, r_1^v,$$

$$(39b) \quad \nabla^j \text{div } \boldsymbol{\tau}(\mathbf{v}), \quad \mathbf{v} \in \Delta_0(T), j = r_1^v, \dots, r_2^v,$$

$$(39c) \quad \int_e (\boldsymbol{\tau} \mathbf{n}) \cdot \mathbf{q} \, ds, \quad \mathbf{q} \in \mathbb{P}_{k-2(r_1^v+1)}^2(e), e \in \Delta_1(T),$$

$$(39d) \quad \int_e \partial_n^i (\mathbf{t}^\top \boldsymbol{\tau} \mathbf{t}) \, q \, ds, \quad \mathbf{q} \in \mathbb{P}_{k-2(r_1^v+1)+i}(e), e \in \Delta_1(T), i = 0, \dots, r_1^e,$$

$$(39e) \quad \int_e \partial_n^i (\text{div } \boldsymbol{\tau}) \cdot \mathbf{q} \, ds, \quad \mathbf{q} \in \mathbb{P}_{k-1-2(r_2^v+1)+i}(e), e \in \Delta_1(T), i = 0, \dots, r_2^e,$$

$$(39f) \quad \int_T \text{div } \boldsymbol{\tau} \cdot \mathbf{q} \, dx, \quad \mathbf{q} \in \mathbb{B}_{k-1}^2(\mathbf{r}_2) / \mathbf{RM},$$

$$(39g) \quad \int_T \boldsymbol{\tau} : \mathbf{q} \, dx, \quad \mathbf{q} \in \text{Air } \mathbb{B}_{k+2}(\mathbf{r}_1 + 2).$$

Lemma 5.3. *The DoFs (39a)-(39g) are uni-solvent for $\mathbb{P}_k(T; \mathbb{S})$.*

Proof. The number of DoFs (39b) and (39e)-(39f) is $2 \dim \mathbb{P}_{k-1}(T) - 3 - 6 \binom{r_1^v+1}{2}$. Then the number of DoFs (39a)-(39g) is

$$\begin{aligned} & 9 \binom{r_1^v+2}{2} + 6(k-1-2r_1^v) + 3 \sum_{i=0}^{r_1^e} (k-1-2r_1^v+i) + \dim \mathbb{B}_{k+2}(\mathbf{r}_1+2) \\ & + 2 \dim \mathbb{P}_{k-1}(T) - 3 - 6 \binom{r_1^v+1}{2} = \dim \mathbb{P}_{k+2}(T) + 2 \dim \mathbb{P}_{k-1}(T) - 3, \end{aligned}$$

by (13), which equals to $\dim \mathbb{P}_k(T; \mathbb{S})$.

Take $\boldsymbol{\tau} \in \mathbb{P}_k(T; \mathbb{S})$, and assume all the DoFs (39a)-(39g) vanish. It follows from the integration by parts and (39c) that

$$(\operatorname{div} \boldsymbol{\tau}, \mathbf{q})_T = 0 \quad \forall \mathbf{q} \in \mathbf{RM}.$$

Thanks to DoFs (39a)-(39b) and (39e)-(39f), we get $\operatorname{div} \boldsymbol{\tau} = \mathbf{0}$. On each edge e ,

$$\begin{aligned} \partial_n^i(\operatorname{div} \boldsymbol{\tau}) &= \partial_n^i(\operatorname{div}(\mathbf{n}^\top \boldsymbol{\tau}))\mathbf{n} + \partial_n^i(\operatorname{div}(\mathbf{t}^\top \boldsymbol{\tau}))\mathbf{t} \\ &= \partial_n^i(\partial_n(\mathbf{n}^\top \boldsymbol{\tau}\mathbf{n}) + \partial_t(\mathbf{n}^\top \boldsymbol{\tau}\mathbf{t}))\mathbf{n} + \partial_n^i(\partial_n(\mathbf{t}^\top \boldsymbol{\tau}\mathbf{n}) + \partial_t(\mathbf{t}^\top \boldsymbol{\tau}\mathbf{t}))\mathbf{t} \\ &= (\partial_n^{i+1}(\mathbf{n}^\top \boldsymbol{\tau}\mathbf{n}) + \partial_t \partial_n^i(\mathbf{n}^\top \boldsymbol{\tau}\mathbf{t}))\mathbf{n} + (\partial_n^{i+1}(\mathbf{t}^\top \boldsymbol{\tau}\mathbf{n}) + \partial_t \partial_n^i(\mathbf{t}^\top \boldsymbol{\tau}\mathbf{t}))\mathbf{t}. \end{aligned}$$

Then we acquire from DoFs (39a)-(39e) that $\boldsymbol{\tau} \in \operatorname{Air} \mathbb{B}_{k+2}(\mathbf{r}_1 + 2)$. Finally we get $\boldsymbol{\tau} = \mathbf{0}$ from the vanishing DoF (39g). \square

Next we define the global finite element space and show it is $\mathbb{V}_k^{\operatorname{div}}(\mathbf{r}_1, \mathbf{r}_2; \mathbb{S})$.

Lemma 5.4. *It holds*

$$\begin{aligned} \mathbb{V}_k^{\operatorname{div}}(\mathbf{r}_1, \mathbf{r}_2; \mathbb{S}) = \mathbb{V} := \{ \boldsymbol{\tau} \in \mathbf{L}^2(\Omega; \mathbb{S}) : \boldsymbol{\tau}|_T \in \mathbb{P}_k(T; \mathbb{S}) \forall T \in \mathcal{T}_h, \\ \text{all the DoFs (39a)-(39e) are single-valued} \}. \end{aligned}$$

Proof. Apparently $\mathbb{V} \subseteq \mathbb{V}_k^{\operatorname{div}}(\mathbf{r}_1, \mathbf{r}_2; \mathbb{S})$. By comparing DoFs and direct computation, we can show $\dim \mathbb{V}_k^{\operatorname{div}}(\mathbf{r}_1, \mathbf{r}_2; \mathbb{S}) = \dim \mathbb{V}$ and the desired result follows. \square

5.3. Finite element divdiv complexes. We first consider the case: the tensor finite element space is continuous. Let $\mathbf{r}_1 \geq 0$ and $\mathbf{r}_2 \geq \max\{\mathbf{r}_1 - 2, -1\}$. We introduce the space $\mathbb{V}_k^{\operatorname{div} \operatorname{div}^+}(\mathbf{r}_1, \mathbf{r}_2; \mathbb{M}) \subseteq \mathbb{V}_k^{\operatorname{div}}(\mathbf{r}_1) \times \mathbb{V}_k^{\operatorname{div}}(\mathbf{r}_1)$ with constraint on $\operatorname{div} \operatorname{div} \boldsymbol{\tau}$. The shape function space is $\mathbb{P}_k(T; \mathbb{M})$ with $k \geq \max\{2r_1^v + 2, 2r_2^v + 3\}$ and DoFs are

$$(40a) \quad \nabla^i \boldsymbol{\tau}(\mathbf{v}), \quad \mathbf{v} \in \Delta_0(T), i = 0, \dots, r_1^v,$$

$$(40b) \quad \nabla^j \operatorname{div} \operatorname{div} \boldsymbol{\tau}(\mathbf{v}), \quad \mathbf{v} \in \Delta_0(T), j = \max\{r_1^v - 1, 0\}, \dots, r_2^v,$$

$$(40c) \quad \int_e \boldsymbol{\tau} \mathbf{n} \cdot \mathbf{q} \, ds, \quad \mathbf{q} \in \mathbb{P}_{k-2(r_1^v+1)}^2(e), e \in \Delta_1(T),$$

$$(40d) \quad \int_e \partial_n^i(\boldsymbol{\tau} \mathbf{t}) \cdot \mathbf{q} \, ds, \quad \mathbf{q} \in \mathbb{P}_{k-2(r_1^v+1)+i}^2(e), e \in \Delta_1(T), i = 0, \dots, r_1^e,$$

$$(40e) \quad \int_e \mathbf{n}^\top \operatorname{div} \boldsymbol{\tau} \mathbf{q} \, ds, \quad \mathbf{q} \in \mathbb{P}_{k-1-2r_1^v}(e), e \in \Delta_1(T),$$

$$(40f) \quad \int_e \partial_n^i(\mathbf{t}^\top \operatorname{div} \boldsymbol{\tau}) \mathbf{q} \, ds, \quad \mathbf{q} \in \mathbb{P}_{k-1-2r_1^v+i}(e), e \in \Delta_1(T), i = 0, \dots, r_1^e - 1,$$

$$(40g) \quad \int_e \partial_n^i(\operatorname{div} \operatorname{div} \boldsymbol{\tau}) \mathbf{q} \, ds, \quad \mathbf{q} \in \mathbb{P}_{k-2-2(r_2^v+1)+i}(e), e \in \Delta_1(T), i = 0, \dots, r_2^e,$$

$$(40h) \quad \int_T \operatorname{div} \boldsymbol{\tau} \cdot \mathbf{q} \, dx, \quad \mathbf{q} \in \operatorname{curl} \mathbb{B}_k(\mathbf{r}_1),$$

$$(40i) \quad \int_T \operatorname{div} \operatorname{div} \boldsymbol{\tau} \mathbf{q} \, dx, \quad \mathbf{q} \in \mathbb{B}_{k-2}(\mathbf{r}_2)/\mathbb{P}_1(T),$$

$$(40j) \quad \int_T \boldsymbol{\tau} : \mathbf{q} \, dx, \quad \mathbf{q} \in \operatorname{curl} \mathbb{B}_{k+1}(\mathbf{r}_1 + 1; \mathbb{R}^2).$$

Lemma 5.5. *Assume $k \geq \max\{2r_1^v + 2, 2r_2^v + 3, 3r_2^e + 6, 6[r_2^e = -1, r_2^v = 1], 4[r_2^e = -1, r_2^v = 0]\}$. The DoFs (40a)-(40j) are uni-solvent for $\mathbb{P}_k(T; \mathbb{M})$.*

Proof. The number of DoFs (40b), (40g) and (40i) is

$$\dim \mathbb{P}_{k-2}(T) - 3 - 3 \binom{r_1^v}{2} = 3 \sum_{i=1}^{r_1^e-1} (k - 2r_1^v + i) + \dim \mathbb{B}_{k-2}(\max\{\mathbf{r}_1 - 2, -1\}) - 3.$$

And the number of DoFs (32a)-(32g) for $\mathbb{V}_k^{\text{div}}(\mathbf{r}_1, \mathbf{r}_1 - 1)$ minus the number of DoFs (40a), (40c)-(40f), (40h) and (40j) is

$$\begin{aligned} & 3 \sum_{i=1}^{r_1^e-1} (k - 2r_1^v + i) + 2 \dim \mathbb{B}_{k-1}(\mathbf{r}_1 - 1) - \dim \mathbb{B}_k(\mathbf{r}_1) - 2 \\ &= 2 \dim \mathbb{P}_{k-1}(T) - \dim \mathbb{P}_k(T) - 6 \binom{r_1^v + 1}{2} + 3 \binom{r_1^v + 2}{2} - 6 \sum_{i=0}^{r_1^e-1} (k - 2r_1^v + i) \\ & \quad + 3 \sum_{i=0}^{r_1^e} (k - 2r_1^v - 1 + i) + 3 \sum_{i=1}^{r_1^e-1} (k - 2r_1^v + i) - 2 \\ &= 2 \dim \mathbb{P}_{k-1}(T) - \dim \mathbb{P}_k(T) - 3 \binom{r_1^v}{2} - 2, \end{aligned}$$

by (13), which equals to $\dim \mathbb{P}_{k-2}(T) - 3 - 3 \binom{r_1^v}{2}$. Hence the number of DoFs (40a)-(40j) equals to $\dim \mathbb{P}_k(T; \mathbb{M})$.

Take $\boldsymbol{\tau} \in \mathbb{P}_k(T; \mathbb{M})$, and assume all the DoFs (40a)-(40j) vanish. Let $\mathbf{v} = \text{div } \boldsymbol{\tau} \in \mathbb{P}_{k-1}(T; \mathbb{R}^2)$. Applying the integration by parts, it follows from (40c) and (40e) that

$$(\text{div } \mathbf{v}, q)_T = (\text{div } \text{div } \boldsymbol{\tau}, q)_T = 0 \quad \forall q \in \mathbb{P}_1(T).$$

Applying Lemma 4.7, i.e. the unsolvence of space $\mathbb{V}_{k-1}^{\text{div}}(\mathbf{r}_1 - 1, \mathbf{r}_2)$, it follows from DoFs (40a)-(40b) and (40e)-(40i) that $\text{div } \boldsymbol{\tau} = \mathbf{v} = \mathbf{0}$. Then $\boldsymbol{\tau} = \text{curl } \mathbf{w}$ with some $\mathbf{w} \in \mathbb{P}_{k+1}(T; \mathbb{R}^2)$. Thanks to Theorem 3.7, we derive $\mathbf{w} = \mathbf{0}$ and $\boldsymbol{\tau} = \mathbf{0}$ from DoFs (40a), (40c)-(40d) and (40j). \square

Define global $H(\text{div div})$ -conforming finite element space

$$\begin{aligned} \mathbb{V}_k^{\text{div div}^+}(\mathbf{r}_1, \mathbf{r}_2; \mathbb{M}) &= \{\boldsymbol{\tau} \in \mathbf{L}^2(\Omega; \mathbb{M}) : \boldsymbol{\tau}|_T \in \mathbb{P}_k(T; \mathbb{M}) \forall T \in \mathcal{T}_h, \\ & \quad \text{all the DoFs (40a)-(40g) are single-valued}\}. \end{aligned}$$

The super-script in div div^+ indicates the smoothness is more than div div -conforming. Indeed we have $\mathbb{V}_k^{\text{div div}^+}(\mathbf{r}_1, \mathbf{r}_2; \mathbb{M}) \subset \mathbf{H}(\text{div}, \Omega; \mathbb{M}) \cap \mathbf{H}(\text{div div}, \Omega; \mathbb{M})$.

Theorem 5.6. *Let $\mathbf{r}_1 \geq 0$ and $\mathbf{r}_2 \geq \max\{\mathbf{r}_1 - 2, -1\}$. Assume $k \geq \max\{2r_1^v + 2, 2r_2^v + 3, 3r_2^e + 6, 6[r_2^e = -1, r_2^v = 1], 4[r_2^e = -1, r_2^v = 0]\}$. The BGG diagram*

$$(41) \quad \begin{array}{ccccccc} \mathbb{R}^2 & \hookrightarrow & \mathbb{V}_{k+1}^{\text{curl}}(\mathbf{r}_1 + 1; \mathbb{R}^2) & \xrightarrow{\text{curl}} & \mathbb{V}_k^{\text{div div}^+}(\mathbf{r}_1, \mathbf{r}_2; \mathbb{M}) & \xrightarrow{\text{div}} & \mathbb{V}_{k-1}^{\text{div}}(\mathbf{r}_1 - 1, \mathbf{r}_2) \rightarrow \mathbf{0} \\ & \nearrow & \searrow & \nearrow & \searrow & \nearrow & \\ & \mathbb{R} & \xrightarrow{\subset} & \mathbb{V}_k^{\text{curl}}(\mathbf{r}_1) & \xrightarrow{\text{curl}} & \mathbb{V}_{k-1}^{\text{div}}(\mathbf{r}_1 - 1, \mathbf{r}_2) & \xrightarrow{\text{div}} & \mathbb{V}_{k-2}^{L^2}(\mathbf{r}_2) \longrightarrow \mathbf{0} \end{array}$$

$\begin{array}{ccc} \text{curl} & \text{mskw} & \text{id} \\ \text{div} & & \end{array}$

which leads to the finite element div div complex

$$(42) \quad \mathbf{RT} \hookrightarrow \mathbb{V}_{k+1}^{\text{curl}}(\mathbf{r}_1 + 1; \mathbb{R}^2) \xrightarrow{\text{sym curl}} \mathbb{V}_k^{\text{div div}^+}(\mathbf{r}_1, \mathbf{r}_2; \mathbb{S}) \xrightarrow{\text{div div}} \mathbb{V}_{k-2}^{L^2}(\mathbf{r}_2) \rightarrow \mathbf{0},$$

where $\mathbb{V}_k^{\text{div div}^+}(\mathbf{r}_1, \mathbf{r}_2; \mathbb{S}) := \mathbb{V}_k^{\text{div div}^+}(\mathbf{r}_1, \mathbf{r}_2; \mathbb{M}) / \text{mskw } \mathbb{V}_k^{\text{curl}}(\mathbf{r}_1)$.

Proof. By the anti-commutative property $\operatorname{div}(\operatorname{mskw} v) = -\operatorname{curl} v$, we can conclude complex (42) from the BGG framework in [7].

In the following we give a self-contained proof without invoking the BGG framework. Clearly (42) is a complex. As $\operatorname{div} \operatorname{div} \operatorname{mskw} \mathbb{V}_k^{\operatorname{curl}}(\mathbf{r}_1) = -\operatorname{div} \operatorname{curl} \mathbb{V}_k^{\operatorname{curl}}(\mathbf{r}_1) = 0$, we have

$$\operatorname{div} \operatorname{div} \mathbb{V}_k^{\operatorname{div} \operatorname{div}^+}(\mathbf{r}_1, \mathbf{r}_2; \mathbb{S}) = \operatorname{div} \operatorname{div} \mathbb{V}_k^{\operatorname{div} \operatorname{div}^+}(\mathbf{r}_1, \mathbf{r}_2; \mathbb{M}) = \mathbb{V}_{k-2}^{L^2}(\mathbf{r}_2).$$

By two complexes in diagram (41), we have

$$\begin{aligned} \dim \mathbb{V}_k^{\operatorname{div} \operatorname{div}^+}(\mathbf{r}_1, \mathbf{r}_2; \mathbb{M}) &= \dim \mathbb{V}_{k+1}^{\operatorname{curl}}(\mathbf{r}_1 + 1; \mathbb{R}^2) + \dim \mathbb{V}_{k-1}^{\operatorname{div}}(\mathbf{r}_1 - 1, \mathbf{r}_2) - 2, \\ \dim \mathbb{V}_{k-1}^{\operatorname{div}}(\mathbf{r}_1 - 1, \mathbf{r}_2) &= \dim \mathbb{V}_k^{\operatorname{curl}}(\mathbf{r}_1) + \dim \mathbb{V}_{k-2}^{L^2}(\mathbf{r}_2) - 1. \end{aligned}$$

Combining the last two equations yields

$$\dim \mathbb{V}_k^{\operatorname{div} \operatorname{div}^+}(\mathbf{r}_1, \mathbf{r}_2; \mathbb{M}) = \dim \mathbb{V}_{k+1}^{\operatorname{curl}}(\mathbf{r}_1 + 1; \mathbb{R}^2) + \dim \mathbb{V}_k^{\operatorname{curl}}(\mathbf{r}_1) + \dim \mathbb{V}_{k-2}^{L^2}(\mathbf{r}_2) - 3.$$

Hence

$$\dim \mathbb{V}_k^{\operatorname{div} \operatorname{div}^+}(\mathbf{r}_1, \mathbf{r}_2; \mathbb{S}) = \dim \mathbb{V}_{k+1}^{\operatorname{curl}}(\mathbf{r}_1 + 1; \mathbb{R}^2) + \dim \mathbb{V}_{k-2}^{L^2}(\mathbf{r}_2) - 3.$$

Therefore the exactness of complex (42) follows from Lemma 2.1. \square

Next we give the finite element characterization of $\mathbb{V}_k^{\operatorname{div} \operatorname{div}^+}(\mathbf{r}_1, \mathbf{r}_2; \mathbb{S})$. We choose $\mathbb{P}_k(T; \mathbb{S})$ as the shape function space. By symmetrizing DoFs (40a)-(40j), we propose the following local DoFs:

$$(43a) \quad \nabla^i \boldsymbol{\tau}(\mathbf{v}), \quad \mathbf{v} \in \Delta_0(T), i = 0, \dots, r_1^v,$$

$$(43b) \quad \nabla^j \operatorname{div} \operatorname{div} \boldsymbol{\tau}(\mathbf{v}), \quad \mathbf{v} \in \Delta_0(T), j = \max\{r_1^v - 1, 0\}, \dots, r_2^v,$$

$$(43c) \quad \int_e \boldsymbol{\tau} \mathbf{n} \cdot \mathbf{q} \, ds, \quad \mathbf{q} \in \mathbb{P}_{k-2(r_1^v+1)}^2(e), e \in \Delta_1(T),$$

$$(43d) \quad \int_e \partial_n^i(\mathbf{t}^\top \boldsymbol{\tau} \mathbf{t}) q \, ds, \quad q \in \mathbb{P}_{k-2(r_1^v+1)+i}(e), e \in \Delta_1(T), i = 0, \dots, r_1^e,$$

$$(43e) \quad \int_e \mathbf{n}^\top \operatorname{div} \boldsymbol{\tau} q \, ds, \quad q \in \mathbb{P}_{k-1-2r_1^v}(e), e \in \Delta_1(T),$$

$$(43f) \quad \int_e \partial_n^i(\mathbf{t}^\top \operatorname{div} \boldsymbol{\tau}) q \, ds, \quad q \in \mathbb{P}_{k-1-2r_1^v+i}(e), e \in \Delta_1(T), i = 0, \dots, r_1^e - 1,$$

$$(43g) \quad \int_e \partial_n^i(\operatorname{div} \operatorname{div} \boldsymbol{\tau}) q \, ds, \quad q \in \mathbb{P}_{k-2(r_2^v+2)+i}(e), e \in \Delta_1(T), i = 0, \dots, r_2^e,$$

$$(43h) \quad \int_T \operatorname{div} \boldsymbol{\tau} \cdot \mathbf{q} \, dx, \quad \mathbf{q} \in \operatorname{curl} \mathbb{B}_k(\mathbf{r}_1) / \mathbf{x}^\perp,$$

$$(43i) \quad \int_T \operatorname{div} \operatorname{div} \boldsymbol{\tau} q \, dx, \quad q \in \mathbb{B}_{k-2}(\mathbf{r}_2) / \mathbb{P}_1(T),$$

$$(43j) \quad \int_T \boldsymbol{\tau} : \mathbf{q} \, dx, \quad \mathbf{q} \in \operatorname{Air} \mathbb{B}_{k+2}(\mathbf{r}_1 + 2).$$

Using a similar proof as that in Lemma 5.5, we can prove the unisolvence.

Lemma 5.7. *Let $r_1 \geq 0$ and $r_2 \geq \max\{r_1 - 2, -1\}$. Assume $k \geq \max\{2r_1^v + 2, 2r_2^v + 3, 3r_2^e + 6, 6[r_2^e = -1, r_2^v = 1], 4[r_2^e = -1, r_2^v = 0]\}$. The DoFs (43a)-(43j) are uni-solvent for $\mathbb{P}_k(T; \mathbb{S})$.*

Lemma 5.8. *Let $\mathbf{r}_1 \geq 0$ and $\mathbf{r}_2 \geq \max\{\mathbf{r}_1 - 2, -1\}$. Assume $k \geq \max\{2r_1^v + 2, 2r_2^v + 3, 3r_2^e + 6, 6[r_2^e = -1, r_2^v = 1], 4[r_2^e = -1, r_2^v = 0]\}$. It holds that*

$$\mathbb{V}_k^{\text{div div}^+}(\mathbf{r}_1, \mathbf{r}_2; \mathbb{S}) = \mathbb{V} := \{\boldsymbol{\tau} \in \mathbf{L}^2(\Omega; \mathbb{S}) : \boldsymbol{\tau}|_T \in \mathbb{P}_k(T; \mathbb{S}) \forall T \in \mathcal{T}_h, \\ \text{all the DoFs (43a)-(43g) are single-valued}\}$$

and $\mathbb{V}_k^{\text{div div}^+}(\mathbf{r}_1, \mathbf{r}_2; \mathbb{S}) \subset \mathbf{H}(\text{div}, \Omega; \mathbb{S}) \cap \mathbf{H}(\text{div div}, \Omega; \mathbb{S})$.

Proof. Apparently $\mathbb{V} \subseteq \mathbb{V}_k^{\text{div div}^+}(\mathbf{r}_1, \mathbf{r}_2; \mathbb{S})$. It suffices to prove $\dim \mathbb{V}_k^{\text{div div}^+}(\mathbf{r}_1, \mathbf{r}_2; \mathbb{S}) = \dim \mathbb{V}$ which can be verified by a direct computation and the Euler's formula. \square

Example 5.9. We choose $\mathbf{r}_1 = (1, 0)$, $\mathbf{r}_2 = (0, 0)$ to get the divdiv complex constructed in [15] for $k \geq 6$

$$\mathbf{RT} \xrightarrow{\subset} \text{Argv}_{k+1}\left(\begin{pmatrix} 2 \\ 1 \end{pmatrix}; \mathbb{R}^2\right) \xrightarrow{\text{sym curl}} \mathbb{V}_k^{\text{div div}^+}\left(\begin{pmatrix} 1 \\ 0 \end{pmatrix}, \begin{pmatrix} 0 \\ 0 \end{pmatrix}; \mathbb{S}\right) \xrightarrow{\text{div div}} \text{Lagrange}_{k-2}\left(\begin{pmatrix} 0 \\ 0 \end{pmatrix}\right) \rightarrow 0.$$

The finite element divdiv complexes presented in [29, 13] with $\mathbf{r}_1 = (0, -1)$, $\mathbf{r}_2 = (-1, -1)$ are not included in complex (42) due to the mis-match of the smoothness. In (41), $\text{sskw}(\boldsymbol{\tau})$ is discontinuous for $\boldsymbol{\tau} \in \mathbb{V}_k^{\text{div}}\left(\begin{pmatrix} r_1^v \\ -1 \end{pmatrix}, \mathbf{r}_2; \mathbb{M}\right)$. The operator mskw is still injective. But it is unclear if $\mathbb{V}_k^{\text{div div}^+}\left(\begin{pmatrix} r_1^v \\ -1 \end{pmatrix}, \mathbf{r}_2; \mathbb{M}\right) / \text{mskw} \mathbb{V}_k^{\text{curl}}\left(\begin{pmatrix} r_1^v \\ 0 \end{pmatrix}\right)$ consists of symmetric matrix functions with desirable normal continuity. The continuous version of the divdiv complex is [29]

$$(44) \quad \mathbf{RT} \xrightarrow{\subset} \mathbf{H}^{1,1}(\text{div}, \Omega) \xrightarrow{\text{sym curl}} \mathbf{H}(\text{div div}, \Omega; \mathbb{S}) \cap \mathbf{H}(\text{div}, \Omega; \mathbb{S}) \xrightarrow{\text{div div}} L^2(\Omega) \rightarrow 0.$$

Now we consider the finite element discretization of the divdiv complex (44) by using the BGG framework. For the case $\mathbf{r}_1 = (r_1^v, -1)$ with $r_1^v \geq 0$, $\mathbf{r}_0 = \mathbf{r}_1 + 1$ and $\mathbf{r}_2 \geq \max\{\mathbf{r}_1 - 2, -1\}$, we refine the BGG diagram (41) to

$$(45) \quad \begin{array}{ccccccc} \mathbb{R}^2 & \xrightarrow{\subset} & \mathbb{V}_{k+1}^{\text{div}}(\mathbf{r}_0, \begin{pmatrix} r_1^v \\ 0 \end{pmatrix}) & \xrightarrow{\text{curl}} & \hat{\mathbb{V}}_k^{\text{div div}^+}(\mathbf{r}_1, \mathbf{r}_2; \mathbb{M}) & \xrightarrow{\text{div}} & \mathbb{V}_{k-1}^{\text{div}}\left(\begin{pmatrix} r_1^v - 1 \\ -1 \end{pmatrix}, \mathbf{r}_2\right) \rightarrow 0 \\ & \nearrow & \nearrow & \nearrow & \nearrow & \nearrow & \nearrow \\ & \text{-}\mathbf{x} & & \text{mskw} & & \text{id} & \\ \mathbb{R} & \xrightarrow{\subset} & \mathbb{V}_k^{\text{curl}}\left(\begin{pmatrix} r_1^v \\ 0 \end{pmatrix}\right) & \xrightarrow{\text{curl}} & \mathbb{V}_{k-1}^{\text{div}}\left(\begin{pmatrix} r_1^v - 1 \\ -1 \end{pmatrix}, \mathbf{r}_2\right) & \xrightarrow{\text{div}} & \mathbb{V}_{k-2}^{L^2}(\mathbf{r}_2) \longrightarrow 0 \end{array}.$$

Here the space $\hat{\mathbb{V}}_k^{\text{div div}^+}(\mathbf{r}_1, \mathbf{r}_2; \mathbb{M})$ is the subspace of $\mathbb{V}_k^{\text{div div}^+}(\mathbf{r}_1, \mathbf{r}_2; \mathbb{M})$ defined by

$$\hat{\mathbb{V}}_k^{\text{div div}^+}(\mathbf{r}_1, \mathbf{r}_2; \mathbb{M}) := \left\{ \boldsymbol{\tau} \in \mathbb{V}_k^{\text{div div}^+}(\mathbf{r}_1, \mathbf{r}_2; \mathbb{M}) : \text{sskw} \boldsymbol{\tau} \in \mathbb{V}_k^{\text{curl}}\left(\begin{pmatrix} r_1^v \\ 0 \end{pmatrix}\right) \right\}.$$

The diagram (45) will lead to the finite element divdiv complex (46) with the finite element space $\mathbb{V}_k^{\text{div div}^+}(\mathbf{r}_1, \mathbf{r}_2; \mathbb{S}) = \hat{\mathbb{V}}_k^{\text{div div}^+}(\mathbf{r}_1, \mathbf{r}_2; \mathbb{M}) / \text{mskw} \mathbb{V}_k^{\text{curl}}\left(\begin{pmatrix} r_1^v \\ 0 \end{pmatrix}\right)$.

Next we prove the exactness of the derived finite element divdiv complex directly rather than using the BGG framework. The space $\mathbb{V}_k^{\text{div div}^+}(\mathbf{r}_1, \mathbf{r}_2; \mathbb{S})$ is still defined by DoFs (43) and recall that $i = 0, \dots, -1$ means empty and thus (43d) and (43f) are not present.

Theorem 5.10. *Let $\mathbf{r}_1 = (r_1^v, -1)$, $r_1^v \geq 0$ and $\mathbf{r}_2 \geq \max\{\mathbf{r}_1 - 2, -1\}$. Assume $k \geq \max\{2r_1^v + 2, 2r_2^v + 3, 3r_2^e + 6, 6[r_2^e = -1, r_2^v = 1], 4[r_2^e = -1, r_2^v = 0]\}$. The following finite element divdiv complex is exact*

(46)

$$\mathbf{RT} \xrightarrow{\subset} \mathbb{V}_{k+1}^{\text{div}} \left(\begin{pmatrix} r_1^v + 1 \\ 0 \end{pmatrix}, \begin{pmatrix} r_1^v \\ 0 \end{pmatrix} \right) \xrightarrow{\text{sym curl}} \mathbb{V}_k^{\text{div div}^+} \left(\begin{pmatrix} r_1^v \\ -1 \end{pmatrix}, \mathbf{r}_2; \mathbb{S} \right) \xrightarrow{\text{div div}} \mathbb{V}_{k-2}^{L^2}(\mathbf{r}_2) \rightarrow 0.$$

Proof. It is easy to check that (46) is a complex. We will prove the exactness of complex (46).

By divdiv complex (42), we have $\text{div div } \mathbb{V}_k^{\text{div div}^+} \left(\begin{pmatrix} r_1^v \\ 0 \end{pmatrix}, \mathbf{r}_2; \mathbb{S} \right) = \mathbb{V}_{k-2}^{L^2}(\mathbf{r}_2)$. Noting that

$$\text{div div } \mathbb{V}_k^{\text{div div}^+} \left(\begin{pmatrix} r_1^v \\ 0 \end{pmatrix}, \mathbf{r}_2; \mathbb{S} \right) \subseteq \text{div div } \mathbb{V}_k^{\text{div div}^+} \left(\begin{pmatrix} r_1^v \\ -1 \end{pmatrix}, \mathbf{r}_2; \mathbb{S} \right) \subseteq \mathbb{V}_{k-2}^{L^2}(\mathbf{r}_2),$$

hence $\text{div div } \mathbb{V}_k^{\text{div div}^+} \left(\begin{pmatrix} r_1^v \\ -1 \end{pmatrix}, \mathbf{r}_2; \mathbb{S} \right) = \mathbb{V}_{k-2}^{L^2}(\mathbf{r}_2)$. On the other side,

$$\begin{aligned} & \dim \mathbb{V}_k^{\text{div div}^+} \left(\begin{pmatrix} r_1^v \\ -1 \end{pmatrix}, \mathbf{r}_2; \mathbb{S} \right) - \dim \mathbb{V}_{k-2}^{L^2}(\mathbf{r}_2) \\ &= 3 \binom{r_1^v + 2}{2} |\Delta_0(\mathcal{T}_h)| - \binom{r_1^v}{2} |\Delta_0(\mathcal{T}_h)| + (3k - 6r_1^v - 2) |\Delta_1(\mathcal{T}_h)| \\ & \quad + |\Delta_2(\mathcal{T}_h)| \dim \mathbb{B}_k \left(\begin{pmatrix} r_1^v \\ 0 \end{pmatrix} \right) + |\Delta_2(\mathcal{T}_h)| \dim \mathbb{B}_{k+2} \left(\begin{pmatrix} r_1^v + 2 \\ 1 \end{pmatrix} \right) - 4 |\Delta_2(\mathcal{T}_h)| \\ &= 2 \binom{r_1^v + 3}{2} |\Delta_0(\mathcal{T}_h)| + (3k - 6r_1^v - 5) |\Delta_1(\mathcal{T}_h)| \\ & \quad + |\Delta_2(\mathcal{T}_h)| \dim \mathbb{B}_k \left(\begin{pmatrix} r_1^v \\ 0 \end{pmatrix} \right) + |\Delta_2(\mathcal{T}_h)| \dim \mathbb{B}_{k+2} \left(\begin{pmatrix} r_1^v + 2 \\ 1 \end{pmatrix} \right) - |\Delta_2(\mathcal{T}_h)| \\ & \quad - 3(|\Delta_0(\mathcal{T}_h)| - |\Delta_1(\mathcal{T}_h)| + |\Delta_2(\mathcal{T}_h)|). \end{aligned}$$

Thanks to the DoFs (32a)-(32g) for $\mathbb{V}_{k+1}^{\text{div}} \left(\begin{pmatrix} r_1^v + 1 \\ 0 \end{pmatrix}, \begin{pmatrix} r_1^v \\ 0 \end{pmatrix} \right)$ and the Euler's formula,

$$\dim \mathbb{V}_k^{\text{div div}^+} \left(\begin{pmatrix} r_1^v \\ -1 \end{pmatrix}, \mathbf{r}_2; \mathbb{S} \right) - \dim \mathbb{V}_{k-2}^{L^2}(\mathbf{r}_2) = \dim \mathbb{V}_{k+1}^{\text{div}} \left(\begin{pmatrix} r_1^v + 1 \\ 0 \end{pmatrix}, \begin{pmatrix} r_1^v \\ 0 \end{pmatrix} \right) - 3,$$

which together with Lemma 2.1 indicates the exactness of complex (46). \square

Example 5.11. When $r_1^v = 0$ and $\mathbf{r}_2 = -1$, we recover the finite element divdiv complex constructed in [29] for $k \geq 3$

$$\mathbf{RT} \xrightarrow{\subset} \mathbb{V}_{k+1}^{\text{div}} \left(\begin{pmatrix} 1 \\ 0 \end{pmatrix}, \begin{pmatrix} 0 \\ 0 \end{pmatrix} \right) \xrightarrow{\text{sym curl}} \text{HMZ}_k \left(\begin{pmatrix} 0 \\ -1 \end{pmatrix} \right) \xrightarrow{\text{div div}} \text{DG}_{k-2} \left(\begin{pmatrix} -1 \\ -1 \end{pmatrix} \right) \rightarrow 0.$$

Another modification is to relax the smoothness $\mathbf{H}(\text{div div}, \Omega; \mathbb{S}) \cap \mathbf{H}(\text{div}, \Omega; \mathbb{S})$ to $\mathbf{H}(\text{div div}, \Omega; \mathbb{S})$ only. We will modify (43) by replacing (43c)-(43f) with

$$(47a) \quad \int_e \mathbf{n}^\top \boldsymbol{\tau} \mathbf{n} q \, ds, \quad q \in \mathbb{P}_{k-2(r_1^v+1)}(e), e \in \Delta_1(T),$$

$$(47b) \quad \int_e \mathbf{t}^\top \boldsymbol{\tau} \mathbf{n} q \, ds, \quad q \in \mathbb{P}_{k-2(r_1^v+1)}(e), e \in \Delta_1(T),$$

$$(47c) \quad \int_e \text{tr}_2^{\text{div div}}(\boldsymbol{\tau}) q \, ds, \quad q \in \mathbb{P}_{k-1-2r_1^v}(e), e \in \Delta_1(T),$$

where $\text{tr}_2^{\text{div div}}(\boldsymbol{\tau}) = \partial_t(\mathbf{t}^\top \boldsymbol{\tau} \mathbf{n}) + \mathbf{n}^\top \text{div } \boldsymbol{\tau}$ is one of the trace operators of div div ; see [13].

Define

$$\mathbb{V}_k^{\text{div div}}\left(\begin{pmatrix} r_1^\vee \\ -1 \end{pmatrix}, \mathbf{r}_2; \mathbb{S}\right) = \mathbb{V} := \{\boldsymbol{\tau} \in \mathbf{L}^2(\Omega; \mathbb{S}) : \boldsymbol{\tau}|_T \in \mathbb{P}_k(T; \mathbb{S}) \forall T \in \mathcal{T}_h,$$

all the DoFs (43) by replacing (43c)-(43f) with (47) except (47b) are single-valued\}.

As $\mathbf{t}^\top \boldsymbol{\tau} \mathbf{n}$ is local, the vector $\boldsymbol{\tau} \mathbf{n}$ is not continuous across edges. But $\text{tr}_1^{\text{div div}}(\boldsymbol{\tau}) = \mathbf{n}^\top \boldsymbol{\tau} \mathbf{n}$ and $\text{tr}_2^{\text{div div}}(\boldsymbol{\tau})$ are continuous. So the space $\mathbb{V}_k^{\text{div div}}\left(\begin{pmatrix} r_1^\vee \\ -1 \end{pmatrix}, \mathbf{r}_2; \mathbb{S}\right) \subset \mathbf{H}(\text{div div}, \Omega; \mathbb{S})$ but not in $\mathbf{H}(\text{div}, \Omega; \mathbb{S})$. It cannot be derived from the BGG diagram (45) as the induced space should be in $\mathbf{H}(\text{div}, \Omega; \mathbb{S})$.

Theorem 5.12. *The following finite element divdiv complex is exact*

$$(48) \quad \mathbf{RT} \xrightarrow{\subset} \mathbb{V}_{k+1}^{\text{curl}}\left(\begin{pmatrix} r_1^\vee + 1 \\ 0 \end{pmatrix}; \mathbb{R}^2\right) \xrightarrow{\text{sym curl}} \mathbb{V}_k^{\text{div div}}\left(\begin{pmatrix} r_1^\vee \\ -1 \end{pmatrix}, \mathbf{r}_2; \mathbb{S}\right) \xrightarrow{\text{div div}} \mathbb{V}_{k-2}^{L^2}(\mathbf{r}_2) \rightarrow 0.$$

Proof. For $\boldsymbol{\tau} = \text{sym curl } \mathbf{v}$, we have [13, Lemma 2.2]

$$\mathbf{n}^\top \boldsymbol{\tau} \mathbf{n} = \partial_t(\mathbf{v} \cdot \mathbf{n}), \quad \text{tr}_2^{\text{div div}}(\boldsymbol{\tau}) = \partial_{tt}(\mathbf{v} \cdot \mathbf{t}).$$

Then it is obvious that (48) is a complex. We will show the exactness of complex (48).

Noting that $\mathbb{V}_k^{\text{div div}^+}\left(\begin{pmatrix} r_1^\vee \\ -1 \end{pmatrix}, \mathbf{r}_2; \mathbb{S}\right) \subseteq \mathbb{V}_k^{\text{div div}}\left(\begin{pmatrix} r_1^\vee \\ -1 \end{pmatrix}, \mathbf{r}_2; \mathbb{S}\right)$, by the exactness of complex (46), we have

$$\text{div div } \mathbb{V}_k^{\text{div div}}\left(\begin{pmatrix} r_1^\vee \\ -1 \end{pmatrix}, \mathbf{r}_2; \mathbb{S}\right) = \mathbb{V}_{k-2}^{L^2}(\mathbf{r}_2).$$

On the other side,

$$\begin{aligned} & \dim \mathbb{V}_k^{\text{div div}}\left(\begin{pmatrix} r_1^\vee \\ -1 \end{pmatrix}, \mathbf{r}_2; \mathbb{S}\right) - \dim \mathbb{V}_{k-2}^{L^2}(\mathbf{r}_2) \\ &= 2 \binom{r_1^\vee + 3}{2} |\Delta_0(\mathcal{T}_h)| + 2(k - 2r_1^\vee - 2) |\Delta_1(\mathcal{T}_h)| \\ & \quad + |\Delta_2(\mathcal{T}_h)| \dim \mathbb{B}_k\left(\begin{pmatrix} r_1^\vee \\ -1 \end{pmatrix}\right) + |\Delta_2(\mathcal{T}_h)| \dim \mathbb{B}_{k+2}\left(\begin{pmatrix} r_1^\vee + 2 \\ 1 \end{pmatrix}\right) - |\Delta_2(\mathcal{T}_h)| \\ & \quad - 3(|\Delta_0(\mathcal{T}_h)| - |\Delta_1(\mathcal{T}_h)| + |\Delta_2(\mathcal{T}_h)|). \end{aligned}$$

Thanks to the DoFs (24a)-(24c) for $\mathbb{V}_{k+1}^{\text{curl}}\left(\begin{pmatrix} r_1^\vee + 1 \\ 0 \end{pmatrix}; \mathbb{R}^2\right)$ and the Euler's formula,

$$\dim \mathbb{V}_k^{\text{div div}}\left(\begin{pmatrix} r_1^\vee \\ -1 \end{pmatrix}, \mathbf{r}_2; \mathbb{S}\right) - \dim \mathbb{V}_{k-2}^{L^2}(\mathbf{r}_2) = \dim \mathbb{V}_{k+1}^{\text{curl}}\left(\begin{pmatrix} r_1^\vee + 1 \\ 0 \end{pmatrix}; \mathbb{R}^2\right) - 3,$$

which together with Lemma 2.1 ends the proof. \square

Example 5.13. When $r_1^\vee = 0$ and $\mathbf{r}_2 = -1$, we recover the finite element divdiv complex constructed in [13] for $k \geq 3$

$$\mathbf{RT} \xrightarrow{\subset} \text{Herm}_{k+1}\left(\begin{pmatrix} 1 \\ 0 \end{pmatrix}; \mathbb{R}^2\right) \xrightarrow{\text{sym curl}} \text{CH}_k\left(\begin{pmatrix} 0 \\ -1 \end{pmatrix}\right) \xrightarrow{\text{div div}} \text{DG}_{k-2}\left(\begin{pmatrix} -1 \\ -1 \end{pmatrix}\right) \rightarrow 0.$$

The first finite element divdiv complex in [11] is based on the distributional divdiv complex

$$\mathbf{RT} \xrightarrow{\subset} \mathbf{H}^1(\Omega; \mathbb{R}^2) \xrightarrow{\text{sym curl}} \mathbf{H}^{-1}(\text{div div}, \Omega; \mathbb{S}) \xrightarrow{\text{div div}} \mathbf{H}^{-1}(\Omega) \rightarrow 0,$$

and not covered in this paper.

6. CONCLUSION AND FUTURE WORK

In recent years, there have been several advancements in the construction of finite element Hessian complexes, elasticity complexes, and divdiv complexes, as documented in [13, 16, 15, 18, 25, 26, 27, 29]. Our primary objective is to extend the BGG construction to finite element complexes, unifying these findings and producing more systematic results. In this work, we have achieved this goal in two dimensions. However, the extension to three dimensions presents several challenges.

One of the challenges is the existence of finite element de Rham complexes with varying degrees of smoothness in three dimensions, which we will discuss in a forthcoming work [14]. Additionally, there is a mismatch in the continuity of Sobolev spaces $H^1(\Omega)$, $H(\text{curl}, \Omega)$, and $H(\text{div}, \Omega)$. The main obstacle to generalizing BGG to the discrete case is the mismatch of tangential or normal continuity of $H(\text{curl})$ or $H(\text{div})$ conforming finite element spaces, respectively. In [7], these spaces are replaced by $H^s(\Omega)$ Sobolev spaces with matching indices s . We will investigate further solutions in our future work. Moreover, edge-type finite elements in three dimensions are the most complex elements and require additional investigation.

To facilitate a clear and effective discussion, we will separate the two-dimensional and three-dimensional cases. Although the two-dimensional case is more straightforward and provides some insight into the three-dimensional case, treating them simultaneously in a simple and effective way is not possible due to the differences between the two cases. For instance, the proof of the div stability $\mathbb{V}_k^{\text{div}}(\mathcal{T}_h; \mathbf{r}_1, \mathbf{r}_2) \xrightarrow{\text{div}} \mathbb{V}_{k-1}^{L^2}(\mathcal{T}_h; \mathbf{r}_2) \rightarrow 0$ can be established by dimension count in 2D, but is much more technical in 3D.

REFERENCES

- [1] J. Argyris, I. Fried, and D. Scharpf. The TUBA family of plate elements for the matrix displacement method. *Aero. J. Roy. Aero. Soc.*, 72:701–709, 1968. 14
- [2] D. Arnold, R. Falk, and R. Winther. Finite element exterior calculus: from Hodge theory to numerical stability. *Bull. Amer. Math. Soc. (N.S.)*, 47(2):281–354, 2010. 1
- [3] D. N. Arnold. *Finite element exterior calculus*. Society for Industrial and Applied Mathematics (SIAM), Philadelphia, PA, 2018. 1, 4
- [4] D. N. Arnold, R. S. Falk, and R. Winther. Differential complexes and stability of finite element methods. II. The elasticity complex. In *Compatible spatial discretizations*, volume 142 of *IMA Vol. Math. Appl.*, pages 47–67. Springer, New York, 2006. 5
- [5] D. N. Arnold, R. S. Falk, and R. Winther. Finite element exterior calculus, homological techniques, and applications. *Acta Numer.*, 15:1–155, 2006. 1, 14
- [6] D. N. Arnold, R. S. Falk, and R. Winther. Geometric decompositions and local bases for spaces of finite element differential forms. *Comput. Methods Appl. Mech. Engrg.*, 198(21-26):1660–1672, 2009. 8, 9
- [7] D. N. Arnold and K. Hu. Complexes from complexes. *Found. Comput. Math.*, 21(6):1739–1774, 2021. 1, 2, 5, 21, 23, 26, 30
- [8] D. N. Arnold and R. Winther. Mixed finite elements for elasticity. *Numer. Math.*, 92(3):401–419, 2002. 5
- [9] I. N. Bernšteĭn, I. M. Gelfand, and S. I. Gelfand. Differential operators on the base affine space and a study of g -modules. In *Lie groups and their representations (Proc. Summer School, Bolyai János Math. Soc., Budapest, 1971)*, pages 21–64, 1975. 5
- [10] J. H. Bramble and M. Zlámal. Triangular elements in the finite element method. *Math. Comp.*, 24:809–820, 1970. 6, 14
- [11] L. Chen, J. Hu, and X. Huang. Multigrid methods for Hellan–Herrmann–Johnson mixed method of Kirchhoff plate bending problems. *Journal of Scientific Computing*, 76(2):673–696, 2018. 29
- [12] L. Chen and X. Huang. Decoupling of mixed methods based on generalized Helmholtz decompositions. *SIAM J. Numer. Anal.*, 56(5):2796–2825, 2018. 1

- [13] L. Chen and X. Huang. Finite elements for divdiv-conforming symmetric tensors. *arXiv preprint arXiv:2005.01271*, 2020. 3, 27, 29, 30
- [14] L. Chen and X. Huang. Finite element de Rham and Stokes complexes in three dimensions. *arXiv preprint arXiv:2206.09525*, 2022. 13, 30
- [15] L. Chen and X. Huang. A finite element elasticity complex in three dimensions. *Math. Comp.*, 91(337):2095–2127, 2022. 3, 22, 27, 30
- [16] L. Chen and X. Huang. Finite elements for div div conforming symmetric tensors in three dimensions. *Math. Comp.*, 91(335):1107–1142, 2022. 30
- [17] M. Chen, J. Huang, and X. Huang. A robust lower order mixed finite element method for a strain gradient elasticity model. *SIAM J. Numer. Anal.*, *arXiv:2210.09552*, 2023. 16
- [18] S. H. Christiansen, J. Gopalakrishnan, J. Guzmán, and K. Hu. A discrete elasticity complex on three-dimensional Alfeld splits. *arXiv preprint arXiv:2009.07744*, 2020. 30
- [19] S. H. Christiansen, J. Hu, and K. Hu. Nodal finite element de Rham complexes. *Numer. Math.*, 139(2):411–446, 2018. 2, 3, 18, 22
- [20] S. H. Christiansen and K. Hu. Finite element systems for vector bundles: Elasticity and curvature. *Found. Comput. Math.*, 2022. 3
- [21] M. Eastwood. A complex from linear elasticity. In *The Proceedings of the 19th Winter School “Geometry and Physics” (Srní, 1999)*, pages 23–29, 2000. 5
- [22] R. S. Falk and M. Neilan. Stokes complexes and the construction of stable finite elements with pointwise mass conservation. *SIAM J. Numer. Anal.*, 51(2):1308–1326, 2013. 2, 16, 20
- [23] R. Fan, Y. Liu, and S. Zhang. Mixed schemes for fourth-order DIV equations. *Comput. Methods Appl. Math.*, 19(2):341–357, 2019. 21
- [24] J. Guzmán and M. Neilan. A family of nonconforming elements for the Brinkman problem. *IMA J. Numer. Anal.*, 32(4):1484–1508, 2012. 2
- [25] J. Hu and Y. Liang. Conforming discrete Gradgrad-complexes in three dimensions. *Math. Comp.*, 90(330):1637–1662, 2021. 30
- [26] J. Hu, Y. Liang, and R. Ma. Conforming finite element divdiv complexes and the application for the linearized Einstein–Bianchi system. *SIAM J. Numer. Anal.*, 60(3):1307–1330, 2022. 30
- [27] J. Hu, Y. Liang, R. Ma, and M. Zhang. New conforming finite element divdiv complexes in three dimensions. *arXiv preprint arXiv:2204.07895*, 2022. 30
- [28] J. Hu, T. Lin, and Q. Wu. A construction of C^r conforming finite element spaces in any dimension. *arXiv:2103.14924*, 2021. 2, 14, 15, 17
- [29] J. Hu, R. Ma, and M. Zhang. A family of mixed finite elements for the biharmonic equations on triangular and tetrahedral grids. *Sci. China Math.*, 64(12):2793–2816, 2021. 3, 27, 28, 30
- [30] K. Hu, Q. Zhang, and Z. Zhang. Simple curl-curl-conforming finite elements in two dimensions. *SIAM J. Sci. Comput.*, 42(6):A3859–A3877, 2020. 2, 21
- [31] M.-J. Lai and L. L. Schumaker. *Spline functions on triangulations*, volume 110. Cambridge University Press, 2007. 14
- [32] Y. Liao, P. Ming, and Y. Xu. Taylor-Hood like finite elements for nearly incompressible strain gradient elasticity problems. *J. Sci. Comput.*, 95(1):Paper No. 4, 2023. 16
- [33] K. A. Mardal, X.-C. Tai, and R. Winther. A robust finite element method for Darcy-Stokes flow. *SIAM J. Numer. Anal.*, 40(5):1605–1631, 2002. 2
- [34] J. Morgan and R. Scott. A nodal basis for C^1 piecewise polynomials of degree $n \geq 5$. *Math. Comput.*, 29:736–740, 1975. 14
- [35] A. Ženíšek. Interpolation polynomials on the triangle. *Numer. Math.*, 15:283–296, 1970. 14

DEPARTMENT OF MATHEMATICS, UNIVERSITY OF CALIFORNIA AT IRVINE, IRVINE, CA 92697, USA
Email address: chenlong@math.uci.edu

CORRESPONDING AUTHOR. SCHOOL OF MATHEMATICS, SHANGHAI UNIVERSITY OF FINANCE AND ECONOMICS, SHANGHAI 200433, CHINA
Email address: huang.xuehai@sufe.edu.cn